

1 **Rebuttal and track-changes manuscript**

2 A probabilistic framework for the cover effect in bedrock erosion

3 Submitted to Earth Surface Dynamics

4 Jens M. Turowski & Rebecca Hodge

5

6 Comments to the Author:

7 First, I would like to thank the reviewers for many constructive comments, and the authors for
8 preparing and submitting a revised version of the manuscript. I think that the manuscript has been
9 improved and it is on the right track.

10 However, that said, I also think that there are places where improvements and clarifications are
11 needed before publication.

12 *We thank the editor for his comments. We have tried to further improve the clarity as much as*
13 *possible.*

14

15 I recommend that the authors at this stage continue revision of the manuscript based on my
16 comments to the revised version of the manuscript. My comments are listed below. In this process,
17 the authors should use any potential there is to shorten the text, in particularly section 3, which I
18 found difficult to read.

19 *We do not think that shortening section 3 would aid the clarity of the paper, and therefore have not*
20 *done so. We think this section contains the most interesting and useful results of the paper. We have,*
21 *however, reworked the text and provided an introduction to what we intend to do there and where*
22 *the significance lies. See below for more details.*

23

24 General comments:

25

26 As a first general comment, I must say that I agree with reviewer 1 in that the detailed level of the
27 math hampers the reading of the paper, and I do not think the authors have done enough to meet
28 the concerns of the reviewer here. In my view, the problem is not the equations themselves, nor is it
29 the number of equations. However, the lengthy deviations are in places poorly motivated, and I had
30 several times to read ahead in the paper to understand where the math was going.

31 *We have added explanatory statements of what we are trying to do to the start of each section to*
32 *prepare the reader for what is to come.*

33

34 It is particularly a problem in section 3, which I think could be significantly shortened, for example by
35 moving the non-dimensional analysis in section 3.1 or the steady-state analysis in section 3.2 to the
36 appendix. In stead, I suggest that more use could be made of the numerical solution to eqn. 13 (Fig.
37 8). Does the numerical solution coupled with intuition not illustrate most points (e.g. line 615, 780-
38 782) made about steady-states and the transient transitions between them? I do not question the
39 validity of the analytical solutions, but I wonder if they represent the best way to communicate your
40 points.

41 *We disagree strongly here. We believe the analytic solutions of the steady state cover and of the time*
42 *scale are the core results of the paper and provide the most useful outcome and have emphasized this*
43 *point in the paper. This comes partly from the history of the subject; the relation between the exposed*
44 *fraction and transport stage, as given in eq. 1 and 2, and later in eq. 27 for our model is the common*
45 *form of the cover function in the literature. We believe it is essential to keep the derivation and*
46 *discussion of this equation in the main text, as it provides the link to previously published material.*
47 *Here, we derive an analytical, physically-based (and mathematically correct) expression of this*
48 *equation for the first time and, again, this is a core result of the paper.*

49 *In our mind, the numerical solution is uninteresting beyond illustrating a simple example and*
50 *preparing the following considerations, as it is always tied to specific cases, while the analytical*
51 *solutions give some general insight into the system behavior. The system time scale in particular*
52 *allows estimates of whether in a given situation, a dynamic solution is necessary or whether cover*
53 *can be calculated with steady state equations. The chapter therefore provides a natural continuation*
54 *of the preceding section. We have reworked the introduction to the section to make clearer the*
55 *intentions and the significance of the derivations. Again, this is a core result of the paper – dynamic*
56 *modelling was so far not possible, and only the steady state equations (mostly eq. 1) have been used,*
57 *although there were hints from field, laboratory and numerical work that these are insufficient and*
58 *the sediment dynamics need to be taken into account.*

59

60 In any case, you need to motivate the analytical solutions more and carefully explain the assumptions
61 made.

62 *At the start of the different sections, we have added motivations for the developments that follow.*

63

64 For example, what is the implication of assuming $q_s=0$ in line 503? Under which conditions can this
65 be assumed, which limitations does the assumption introduce, and what new insights can expect
66 from studying this situation in particular.

67 *Here a full analytical solution can be obtained. As it has already been said the past versions, the*
68 *situation is not common in nature, but provides a simple laboratory test for the theory. This can be*
69 *used for example to constrain the P-function.*

70

71 Also, like reviewer 1, I was confused about Eqn. 13. At first glance it looks like a standard continuity
72 equation, but with double treatment of deposition/entrainment. I fully understand the reviewer's
73 comment, and it was only after reading your answer to the reviewer's comment that I understood
74 that this is the balance of only the mobile mass. When introducing the equation in line 314 you write:
75 "...we use the total sediment mass on the bed as a variable". I recommend rephrasing this and
76 explain carefully how the two reservoirs interact. I also recommend including a schematic figure as
77 you suggest, and to move Eqn. 16 up next to Eqn. 13 so that both balance equations for the two
78 sediment reservoirs are presented together. It is important here to carefully present the model to a
79 wide group of readers, instead of relying on the readers' knowledge of the Exner equation (which I
80 did not know, and would not have remembered if I did).

81 *We have reworked the introduction to the chapter and tried to explain the framework better. In*
82 *addition, we have included a cartoon and the mass balance difference equation. We have also*
83 *reorganized the equations, as suggested.*

84

85 Section 2 presents the probabilistic framework, and this section already reads well. However, there
86 are some issues with the implied relation between M_s and Q_s . This relation is the main subject of
87 section 3, but it seems here that you are assuming something that the readers are not yet shown. For
88 example in line 155, you link eq. 6 directly to eq. 1 even though one is using Q_s and the other is using
89 M_s . I failed to see why these two linear equations are identical. At least some clarification is
90 needed.

91 *We agree that we have not been careful in making connections here and have removed them.*

92

93 Like for section 3, I suggest that you consider introducing a simple schematic figure also in section 2,
94 perhaps of an evolving bed-cover in a channel. Such a figure could be used to illustrate the meaning
95 of A^* , M_s^* , P etc. It would also nicely supplement the many curves presented in the other figures.

96 *We added a cartoon. Hopefully this makes things clearer.*

97
98 As a final general comment, there is a tendency in the manuscript to use quite subjective, and at the
99 same time imprecise, descriptions of previous work. Some examples:
100 Line 720: “Despite short-comings, Aubert et al. (2015) presented...” What shortcoming? You need to
101 either skip the reference to shortcomings or carefully describe them.
102 Line 749: “While the model is interesting and provides...” What is interesting about it? Be more
103 specific please, or skip the descriptive wording.
104 Line 771: “...quickly in response to changing boundary conditions, a somewhat counter-intuitive
105 notion for slowly-eroding channels” – If this is counter-intuitive or not must depend on the precise
106 meaning of “quickly” and “slowly-eroding”. Again be more specific or skip it.
107 *We have removed or rewritten these parts.*
108
109 More specific comments:
110
111 line 24: “they” -> channels
112 *Changed to passive mode, ‘such that the supplied sediment load can just be transported’.*
113
114 line 79: “tended” – tend
115 *Changed.*
116
117 lines 99-101: consider rephrasing this sentence; I’m not sure that I understand it.
118 *Sentence has been rephrased; now it reads ‘Using the CA model of Hodge and Hoey (2012), Hodge (in*
119 *press) found that, when sediment supply was very variable (alternating large pulses with no sediment*
120 *supply), the amount of sediment cover was primarily determined by the recent supply history, rather*
121 *than by the relationships identified under constant sediment supply.’*
122
123 lines 124-128: You could move some of the information given in lines 678-698 up here to better
124 motivate why influence of other parameters such as bed topography and roughness is ignored.
125 *To us it seems that this information only makes sense after one has been exposed to the dynamic*
126 *model developed in section 3. Instead, we argue that dealing with A^* only is sufficiently flexible, since*
127 *in the end all the other influences affect the development of A^* .*
128
129 line 162: move “,k,” up to after “...value”; it will make k more visible.
130 *Changed.*
131
132 eq. 9: in eq. 2 you use exp here e – needs to be consistent.
133 *Changed to the exponential notation here. Although, both notations are standard and common, and*
134 *they are defined in the text.*
135
136 line 245: “though” -> “through”?
137 *Corrected.*
138
139 line 254: What is the model step length? Also is the probability of deposition always 1? If so, please
140 write so explicitly.
141 *Text updated to clarify this; now reads ‘In each time step random numbers and the probabilities are*
142 *used to select the grains that are entrained, which are then moved a step length of ten cells*
143 *downstream and deposited. Model results are insensitive to the step length.’*
144

145 line 270: "... given out by the model..." please rephrase.
146 *Rephrased; now 'Cover bed fraction and total mass on the bed produced by the model were converted*
147 *using eq. (3) into the new probabilistic framework (Fig. 3).'*
148
149 line 271: Is the CA model not also a probabilistic model? Its control parameters seem to be
150 likelihoods of entrainment, whereas the "probabilistic framework" presented has likelihoods of
151 deposition. But still, in essence both are probabilistic, right?
152 *Yes, the CA model is also probabilistic, and this is explained in the earlier section. We do not think this*
153 *needs to be further emphasized here.*
154
155 Fig. 3: The comments above also makes me think that there should be more direct relationships
156 between P and A within your framework, and then p_i and p_c from the CA model?
157 *Clearly there is a relation between cover and p_i and p_c , since the latter two variables determine the*
158 *evolution and steady state value of the former. However, it is not possible to derive these relations*
159 *analytically. The 'empirical' connections are depicted in Fig. 3.*
160
161 Line 298: The relation between Q_s^* and M_s is not clear from eqn. 3.
162 *We have removed this reference.*
163
164 Line 299: what do you mean by "muddled"?
165 *We removed this sentence.*
166
167 Line 299: what is incorrect?
168 *We removed this sentence.*
169
170 line 300: "bases" -> "basis"
171 *Corrected.*
172
173 line 312: skip "of course"
174 *Deleted.*
175
176 line 325: while non-dimensional variables are certainly useful, they also introduce complexity. I did
177 not understand why they were necessary here. Please motivate the non-dimensional analysis better.
178 Give the reader some clear hints as to where the analysis is going (and consider moving it to
179 appendix).
180 *We do not think anything is gained by moving the dimensionless variables to the appendix. When the*
181 *equations are written with them, they need to be introduced in the main text and defined anyway,*
182 *and there is little more than that done in the text at the moment.*
183
184 line 335: "The rate of change of the stationary sediment mass..." seems a bit counter-intuitive text-
185 wise. To me "stationary" means "not moving". Could you replace "stationary sediment" with
186 "deposited sediment"? You would have to change this throughout the text though – but the reading
187 would be better I think.
188 *We disagree. The term 'deposited' makes a statement about the history of the sediment and we think*
189 *that 'stationary' is both clearer and more precise. The erosion-deposition framework that we exploit*
190 *here is well established in the theoretical fluvial geomorphology. A stationary particle becomes*
191 *mobile by entrainment and a mobile particle becomes stationary by deposition. We do not think that*

192 *the use of language as we have used it would be confusing to any fluvial geomorphologist and have*
193 *left the terminology as is.*
194
195 line 497: “the equations” – which ones?
196 *Added equation numbers.*
197
198 line 503: Please remind the reader about the meaning of q_s^* and q_t^* . What is happening when $q_s^*=0$
199 and what is the relevance of this case?
200 *We provided an introduction to this chapter, explaining the motivation and significance and moved*
201 *the motivation for the specific case to the beginning of the section.*
202
203 line 663: “1000s” -> “1000 s”
204 *Changed.*
205
206 line 717: “depended” -> “depends” (if Aubert et al.’s results are still valid then consider using present
207 tense in such places.
208 *Changed.*
209
210 line 730-735: I could not follow these arguments about grain size and grid size.
211 *If the grid size is equal to the grain size, each deposited grain covers an entire grid square. If the*
212 *grains are smaller than the grid size, then the distribution of grains within each node determine the*
213 *overall cover.*
214 *We have added explanation: ‘Further, Nelson and Seminara (2011, 2012) assumed a direct*
215 *correspondence between sediment concentration and degree of cover, which is equivalent to the*
216 *linear cover function (eq. 6). In this case, it is assumed that grains are always deposited on uncovered*
217 *bed and the different possible distributions of particles within a grid node are not taken into account.*
218 *Practically, this implies that the grid size needs to be of the order of the grain size, because, strictly,*
219 *the assumption is only valid if a single grain can cover an entire grid node.’*
220
221 line 751-753: I’m still not sure how this would work. Can you be more specific in how bed roughness
222 could be implemented in the framework?
223 *The P-function can be dependent on roughness (see also the statements following its introduction in*
224 *eq. 3). We added a statement to the sentence:*
225 *‘In principle, the probabilistic framework presented here should be able to deal with macro-rough*
226 *beds, by making the P-function (eq. 3) explicitly dependent on roughness, and thus allows a more*
227 *general treatment of the problem of bed cover.’*
228
229 line 762: Also here you could be more precise. It is a general point of this manuscript that the
230 probabilistic framework can be integrated with many types of data, but I’m still not sure how. More
231 guidance would be useful.
232 *If data on stationary sediment mass and cover is available for various steady cover states, one can*
233 *just take the derivative according to eq. 3 and derive P from that. It does not matter whether the data*
234 *were derived from the field, or from laboratory or numerical experiments. The example in section 2.2*
235 *was put in to illustrate this. The process of conversion was explained in the first sentences of the last*
236 *paragraph of this section (starting line 270 in the old version of the manuscript and line 275 in the*
237 *new version).*
238 *Nevertheless, we agree that the statement sits somewhat oddly at the point of the discussion referred*
239 *to here and have removed it.*

240
241 line 771: "Cln" – "In"
242 *Corrected.*
243

244 **-A probabilistic framework for the cover effect in bedrock erosion**

245

246

247 Jens M. Turowski

248 *Helmholtzzentrum Potsdam, German Research Centre for Geosciences GFZ, Telegrafenberg, 14473*

249 *Potsdam, Germany, turowski@gfz-potsdam.de*

250 Rebecca Hodge

251 *Department of Geography, Durham University, Durham, DH1 3LE, United Kingdom,*

252 *rebecca.hodge@durham.ac.uk*

253

254

255 **Abstract**

256 The cover effect in fluvial bedrock erosion is a major control on bedrock channel morphology and long-
257 term channel dynamics. Here, we suggest a probabilistic framework for the description of the cover
258 effect that can be applied to field, laboratory and modelling data and thus allows the comparison of
259 results from different sources. The framework describes the formation of sediment cover as a function
260 of the probability of sediment being deposited on already alluviated areas of the bed. We define
261 benchmark cases and suggest physical interpretations of deviations from these benchmarks.
262 Furthermore, we develop a reach-scale model for sediment transfer in a bedrock channel and use it to
263 clarify the relations between the sediment mass residing on the bed, the exposed bedrock fraction and
264 the transport stage. We derive system time scales and investigate cover response to cyclic
265 perturbations. The model predicts that bedrock channels achieve grade in steady state by adjusting
266 bed cover. Thus, bedrock channels have at least two characteristic time scales of response. Over short
267 time scales, the degree of bed cover is adjusted such that the supplied sediment load can just be
268 transported, while over long time scales, channel morphology evolves such that the bedrock incision
269 rate matches the tectonic uplift or base level lowering rate.

270

271 **1. Introduction**

272

273 Bedrock channels are shaped by erosion caused by countless impacts of the sediment particles they
274 carry along their bed (Beer and Turowski, 2015; Cook et al., 2013; Sklar and Dietrich, 2004). There are
275 feedbacks between the evolving channel morphology, the bedload transport, and the hydraulics
276 (e.g., Finnegan et al., 2007; Johnson and Whipple, 2007; Wohl and Ikeda, 1997). Impacting bedload
277 particles driven forward by the fluid forces erode and therefore shape the bedrock bed. In turn, the
278 morphology of the channel determines the pathways of both sediment and water, and the forces the
279 latter exerts on the former, and thus sets the stage for the entrainment and deposition of the
280 sediment (Hodge and Hoey, 2016). Sediment particles play a key role in this erosion process; they
281 provide the tools for erosion and also determine where bedrock is exposed such that it can be worn
282 away by impacting particles (Gilbert, 1877; Sklar and Dietrich, 2004).

283

284 The importance of the cover effect --that a stationary layer of gravel can shield the bedrock from
285 bedload impacts -- has by now been firmly established in a number of field and laboratory studies
286 (e.g., Chatanantavet and Parker, 2008; Finnegan et al., 2007; Hobbey et al., 2011; Johnson and
287 Whipple, 2007; Turowski and Rickenmann, 2009; Turowski et al., 2008; Yanites et al., 2011).
288 Sediment cover is generally modelled with generic relationships that predict the decrease of the
289 fraction of exposed bedrock area A^* with the increase of the relative sediment supply Q_s^* , usually
290 defined as the ratio of sediment supply to transport capacity. Based on laboratory experiments and
291 simple modeling, Turowski and Bloem (2016) argued that the focus on covered area is generally

292 justified on the reach scale and that erosion of bedrock under a thin sediment cover can be
293 neglected. However, the behavior of sediment cover under flood conditions is currently unknown
294 and the assumption that the cover distribution at low flow is representative ~~offer~~ that at high flow
295 may not be justified (cf. Beer et al., 2016; Turowski et al., 2008).

296

297 The most commonly used function to describe the cover effect is the linear decline (Sklar and
298 Dietrich, 1998), which is the simplest function connecting the steady state end members of an empty
299 bed when relative sediment supply $Q_s^* = 0$ and full cover when $Q_s^* = 1$:

300

$$301 \quad A^* = \begin{cases} 1 - Q_s^* & \text{for } Q_s^* < 1 \\ 0 & \text{otherwise} \end{cases}$$

302 (eq. 1)

303 In contrast, the exponential cover function arises under the assumption that particle deposition is
304 equally likely for each part of the bed, whether it is covered or not (Turowski et al., 2007).

305

$$306 \quad A^* = \begin{cases} e^{-Q_s^*} \exp(-Q_s^*) & \text{for } Q_s^* < 1 \\ 0 & \text{otherwise} \end{cases}$$

307 (eq. 2)

308 Here, ~~exp~~ e is the base of ~~denotes~~ the natural ~~exponential function~~ logarithm.

309

310 Hodge and Hoey (2012) obtained both the linear and the exponential functions using a cellular
311 automaton (CA) model that modulated grain entrainment probabilities by the number of
312 neighbouring grains. However, consistent with laboratory flume data, the same model also produced
313 other behaviours under different parameterisations. One alternative behavior is runaway alluviation,
314 which was attributed by Chatanantavet and Parker (2008) to the differing roughness of bedrock and
315 alluvial patches. Due to a decrease in flow velocity, an increase in surface roughness and differing
316 grain geometry, the likelihood of deposition is higher over bed sections covered by alluvium
317 compared to smooth, bare bedrock sections (Hodge et al., 2011). This can lead to rapid alluviation of
318 the entire bed once a minimum fraction has been covered. The relationship between sediment flux
319 and cover is also affected by the bedrock morphology; flume experiments have demonstrated that
320 on a non-planar bed the location of sediment cover is driven by bed topography and hydraulics (e.g.,
321 Finnegan et al., 2007; Inoue et al., 2014). Johnson and Whipple (2007) ~~found~~ observed that stable
322 patches of alluvium tend to form in topographic lows such as pot holes and at the bottom of slot
323 canyons, whereas Hodge and Hoey (2016) found that local flow velocity also controls sediment cover
324 location.

325

326 The relationship between roughness, bed cover and incision was explored in a number of recent
327 numerical modeling studies. Nelson and Seminara (2011, 2012) were one of the first to model the
328 impact that the differing roughness of bedrock and alluvial areas has on sediment patch stability.
329 Zhang et al. (2014) formulated a macro-roughness cover model, in which sediment cover is related to
330 the ratio of sediment thickness to bedrock macro-roughness. Aubert et al. (2016) directly simulated
331 the dynamics of particles in a turbulent flow and obtained both linear and exponential cover
332 functions. Johnson (2014) linked ~~sediment transport erosion~~ and cover to bed roughness in a reach-
333 scale model. Using a model formulation similar to that of Nelson and Seminara (2011), Inoue et al.
334 (2016) reproduced bar formation and sediment dynamics in bedrock channels. All of these studies
335 used slightly different approaches and mathematical formulations to describe alluvial cover, making
336 a direct comparison difficult.

337

338 Over time scales including multiple floods, the variability in sediment supply is also important (e.g.,
 339 Turowski et al., 2013). Lague (2010) used a model formulation in which cover was written as a
 340 function of the average sediment depth to upscale daily incision processes to long time scales. He
 341 found that over the long term, cover dynamics are largely independent of the precise formulation at
 342 the process scale and are rather controlled by the magnitude-frequency distribution of discharge and
 343 sediment supply. Using the CA model of Hodge and Hoey (2012), Hodge (in press) found that, when
 344 sediment supply was very variable (~~alternating large pulses and with no sediment supply~~), the
 345 amount of sediment cover was primarily determined by the recent ~~supply history of sediment supply~~,
 346 rather than ~~by~~ the relationships identified under constant sediment ~~fluxes supply~~.

347
 348 So far, it has been somewhat difficult to compare and discuss the different cover functions obtained
 349 from theoretical considerations, numerical models, and experiments, since a unifying framework and
 350 clear benchmark cases have been missing. Here, we propose such a framework, and develop type
 351 cases linked to physical considerations of the flow hydraulics and sediment erosion and deposition.
 352 We show how this framework can be applied to data from a published model (Hodge and Hoey,
 353 2012). Furthermore, we develop a reach-scale erosion-deposition model that allows the dynamic
 354 modeling of cover and prediction of steady states. Thus, we clarify the relationship between cover,
 355 deposited mass and relative sediment supply. As part of this model framework we investigate the
 356 response time of a channel to a change in sediment input, which we illustrate using data from a
 357 natural channel.

358 2. A probabilistic framework

359 2.1. Development

360
 361 Here we build on the arguments put forward by Turowski et al. (2007) and Turowski (2009). Consider
 362 a bedrock bed on which sediment particles are distributed. We can view the deposition of each
 363 particle as a random process, and each area element on the bed surface can be assigned a probability
 364 for the deposition of a particle. When assuming that a given number of particles are distributed on
 365 the bed, the mean behavior of the exposed area A^* can be calculated from the following equation
 366 (Fig. 1):

$$367 \quad dA^* = -P(A^*, M_s^*, \dots) dM_s^*$$

368 (eq. 3)

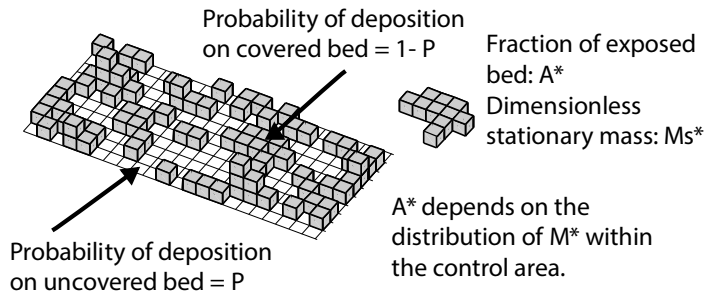
369 P is the probability that a given particle is deposited on the exposed part of the bed, which here is a
 370 function of the fraction of exposed area (A^*) and a dimensionless mass of particles on the bed per
 371 area (M_s^* , explained below), but which can be expected to also be a function of the relative sediment
 372 supply, the bed topography and roughness, the particle size, the local hydraulics or other control
 373 variables. M_s^* is a dimensionless mass equal to the total mass of the particles residing on the bed per
 374 area, which is suitably normalized. A suitable mass for normalization is the minimum mass required
 375 to cover a unit area, M_0 , as will become clear later. The minus sign is introduced because the fraction
 376 of the exposed area reduces as M_s^* increases. ~~Similar to eq. (3), the equation for the fraction of~~
 377 ~~covered area $A_e^* = 1 - A^*$ can be written as:~~

$$378 \quad \cancel{dA_e^* = P(A^*, M_s^*, \dots) dM_s^*}$$

379
 380 (eq. 4)

381 As most previous relationships are expressed in terms of relative sediment supply Q_s^* , the relation of
 382 M_s^* to Q_s^* will be discussed later.

383
 384



385
386 **Fig. 1: Cartoon illustration of a bed partially covered by sediment. For purpose of illustration, the bed**
387 **is divided into a square raster, with each pixel of the size of a single grain. For a given number of**
388 **particles in the area of the bed of interest, the exposed area fraction of the bed is dependent on the**
389 **distribution of particles. Grains that sit on top of other grains do not contribute to cover. The**
390 **probability that a new grain is deposited on uncovered bed is given by P (eq. 3).**
391

392 We can make some general statements about P . First, P is defined for the range $0 \leq A^* \leq 1$ and
393 undefined elsewhere. Second, P takes values between zero and one for $0 \leq A^* \leq 1$. Third, $P(A^*=0) = 0$
394 and $P(A^*=1) = 1$. Note that P is not a distribution function and therefore does not need to integrate
395 to one. Neither does it have to be continuous and differentiable everywhere.

396
397 For purpose of illustration, we will next discuss two simple forms of the probability function P that
398 lead to the linear and exponential forms of the cover effect, respectively. First, consider the case that
399 all particles are always deposited on exposed bedrock. In this case, formally, to keep with the
400 conditions stated above, we define $P = 1$ for $0 < A^* \leq 1$ and $P = 0$ for $A^* = 0$. Thus, we can write
401

$$402 \quad \begin{aligned} dA^* &= -dM_s^* & \text{for } 0 < A^* \leq 1 \\ dA^* &= 0 & \text{for } A^* = 0 \end{aligned}$$

403 (eq. 54)

404 Integrating, we obtain:

$$405 \quad A^* = -M_s^* + C$$

406 (eq. 65)

407 where the constant of integration C is found to equal one by using the condition $A^*(M_s^*=0) = 1$. Thus,
408 we obtain ~~the a~~ linear cover function ~~of eq. (1)~~. Note that the linear cover function gives a theoretical
409 lower bound for the amount of cover: it arises when all available sediment always falls on uncovered
410 ground, and thus no additional sediment is available that could facilitate quicker alluviation. In
411 essence, this is a mass conservation argument. Now it is obvious why M_0 is a convenient way to
412 normalize: in plots of A^* against M_s^* , we obtain a triangular region bounded by the points $[0,1]$, $[0,0]$
413 and $[1,0]$ in which the cover function cannot exist (Fig. 12).
414

415 Similarly to above, if we set P to a constant value, k , smaller than one for $0 < A^* \leq 1$, we obtain
416

$$417 \quad A^* = 1 - kM_s^*$$

418 (eq. 76)

419 It is clear that the assumption of $P = k$ is physically unrealistic, because it implies that the probability
420 of deposition on exposed ground is independent of the amount of uncovered bedrock. Especially
421 when A^* is close to zero, it seems unlikely that, say, always 90% of the sediment falls on uncovered
422 ground. A more realistic assumption is that the probability of deposition on uncovered ground is
423 independent of location and other possible controls, but is equal to the fraction of exposed area, i.e.,
424 $P = A^*$. In a probabilistic sense, this is also the simplest plausible assumption one can make. Then
425

426
$$dA^* = -A^* dM_s^*$$

427 (eq. 87)

428 giving upon integration

429
$$A^* = e^{-M_s^*} \exp(-M_s^*)$$

430 (eq. 98)

431 The argument used here to obtain the exponential cover effect in eq. (98) essentially corresponds to
 432 the one given by Turowski et al. (2007). Since this case presents the simplest plausible assumption,
 433 we will use it as a benchmark case, to which we will compare other possible functional forms of P .

434
 435 In principle, the probability function P can be varied to account for various processes that make
 436 deposition more likely either on already covered ground by decreasing P for the appropriate range of
 437 A^* from the benchmark case $P = A^*$, or on uncovered ground by increasing P from the benchmark
 438 case $P = A^*$. As has been identified previously (Chatanantavet and Parker, 2008; Hodge and Hoey
 439 2012), roughness feedbacks to the flow can cause either case depending on whether subsequent
 440 deposition is adjacent to or on top of existing sediment patches. In the former case, particles residing
 441 on an otherwise bare bedrock bed act as obstacles for moving particles, and create a low-velocity
 442 wake zone in the downstream direction. In addition, particles residing on other single particles are
 443 unstable and stacks of particles are unlikely. Hence, newly arriving particles tend to deposit either
 444 upstream or downstream of stationary particles and the probability is generally higher for deposition
 445 on uncovered ground than in the benchmark case. In the latter case, larger patches of stationary
 446 particles increase the surface roughness of the bed, thus decreasing the local flow velocity and
 447 stresses, making deposition on the patch more likely. In this way, the probability of deposition on
 448 already covered bed is increased in comparison to the benchmark case.

449
 450 A simple functional form that can be used to take into account either one of these two effects is a
 451 power law dependence of P on A^* , taking the form $P = A^{*\alpha}$ (Fig. 1A2A). Then, the cover function
 452 becomes (Fig. 1B2B):

453
 454
$$A^* = (1 - (1 - \alpha)M_s^*)^{\frac{1}{1-\alpha}}$$

455 (eq. 109)

456 Here, the probability of deposition on uncovered ground is increased in comparison to the
 457 benchmark exponential case if $0 < \alpha < 1$, and decreased if $\alpha > 1$.

458
 459 A convenient and flexible way to parameterize $P(A^*)$ in general is the cumulative version of the Beta
 460 distribution, given by:

461
$$P(A^*) = B(A^*; a, b)$$

462 (eq. 1110)

463 Here, $B(A^*; a, b)$ is the regularized incomplete Beta function with two shape parameters a and b ,
 464 which are both real positive numbers, defined by:

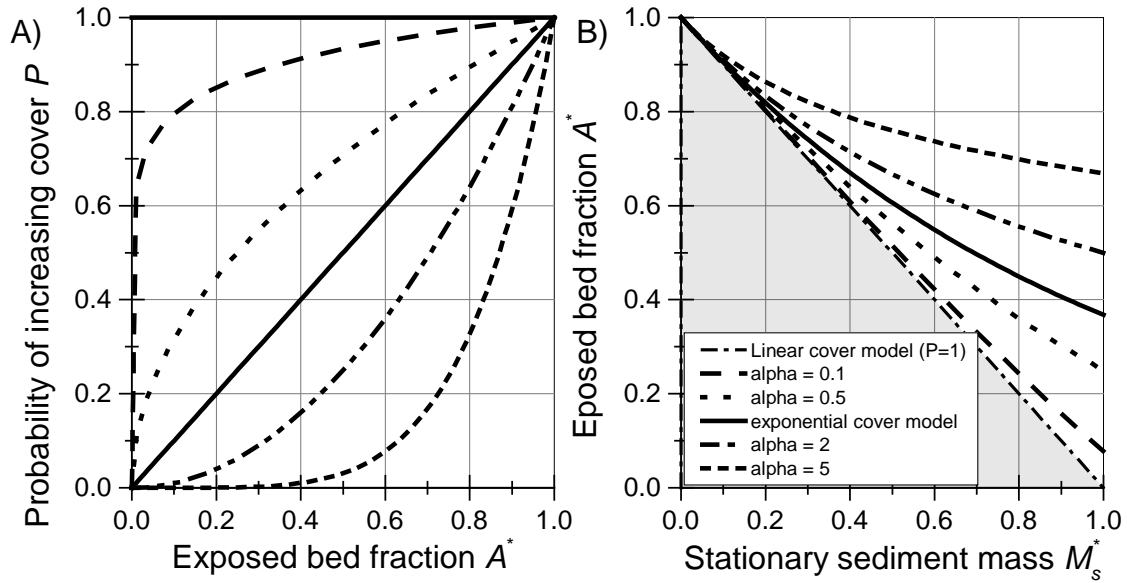
465
$$B(A^*; a, b) = \frac{\int_0^{A^*} y^{a-1} (1-y)^{b-1} dy}{\int_0^1 y^{a-1} (1-y)^{b-1} dy}$$

466 (eq. 1211)

467 Here, y is a dummy variable. With suitable choices for a and b , cover functions resembling the
 468 exponential ($a=b=1$), the linear form ($a=0, b>0$), and the power law form ($a \gg b$ or $a \ll b$) can be
 469 retrieved. Wavy functions are also a possibility (Fig. 23), thus both of the roughness effects described
 470 above can be modelled in a single scenario. Unfortunately, the integral necessary to obtain $A^*(M_s^*)$
 471 does not give a closed-form analytical solution and needs to be computed numerically.

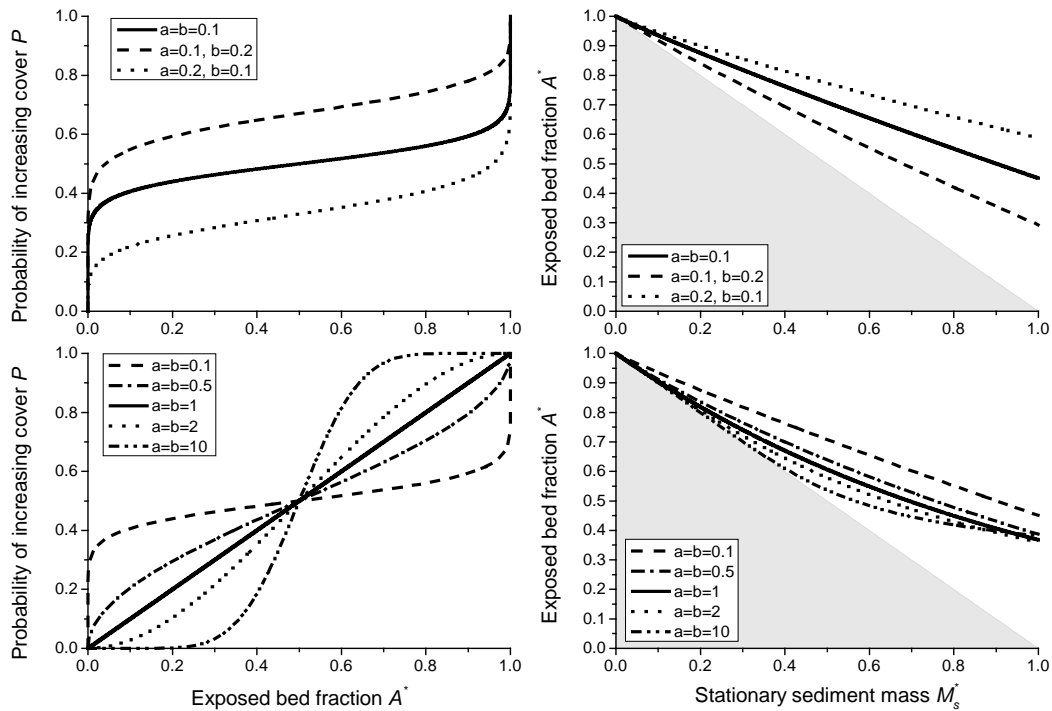
472
 473
 474
 475
 476
 477

In principle, a suitable function P could also be defined to account for the influence of bed topography on sediment deposition. Such a function is likely dependent on the details of the particular bed, hydraulics and sediment flow paths in a complex way and needs to be mapped out experimentally.



478
 479
 480
 481
 482
 483

Fig. 12: A) Various examples for the probability function P as a function of bedrock exposure A^* . B) Corresponding analytical solutions for the cover function between A^* and dimensionless sediment mass M_s^* using eq. (76), (97) and (109). Grey shading depicts the area where the cover function cannot run due to conservation of mass.



484
 485 Fig. 23: Examples for the use of the regularized incomplete Beta function (eq. 4211) to parameterize
 486 P , using various values for the shape parameters a and b . The choice $a = b = 1$ gives a dependence
 487 that is equivalent to the exponential cover function. Grey shading depicts the area where the cover
 488 function cannot run due to conservation of mass.

489
 490 **2.2 Example of application using model data**

491
 492 To illustrate how the framework can be used, we apply it to data obtained from the CA model
 493 developed by Hodge and Hoey (2012). The CA model reproduces the transport of individual sediment
 494 grains over a smooth bedrock surface. In each time step, the probability of a grain being entrained is
 495 a function of the number of neighboring grains. If five or more of the eight neighbouring cells contain
 496 grains then the grain has probability of entrainment p_c , otherwise it has probability p_i . In most model
 497 runs p_c was set to a value less than that of p_i , thus accounting for the impact of sediment cover in
 498 decreasing local shear stress (through increased flow resistance) and increasing the critical
 499 entrainment shear stress for grains (via lower grain exposure and increased pivot angles). Thus, in
 500 the model, grain scale dynamics of entrainment are varied by adjusting the values of p_i and p_c . This
 501 has a direct effect on the reach-scale distribution of cover, which is captured by our P -function (eq.
 502 3).

503
 504 The model is run with a domain that is 100 cells wide by 1000 cells long, with each cell having the
 505 same area as a grain. Up to four grains can potentially be entrained from each cell in a time step,
 506 limiting the maximum sediment flux. In each time step random numbers and the probabilities are
 507 used to select the grains that are entrained, which are then moved a step length of ten cells
 508 downstream and deposited. (Model results are not insensitive to the step length.) A fixed number of
 509 grains are also supplied to the upstream end of the model domain. A smoothing algorithm is applied
 510 to prevent unrealistically tall piles of grains developing in cells if there are far fewer grains in adjacent
 511 cells. After around 500 time steps the model typically reaches a steady state condition in which the

512 number of grains supplied to and leaving the model domain are equal. Sediment cover is measured
 513 in a downstream area of the model domain and is defined as grains that are not entrained in a given
 514 time step. Consequently grains that are deposited in one time step, and entrained in the following
 515 one do not contribute to the sediment cover, and so the model implicitly incorporates the effect of
 516 local sediment cover on grain deposition.

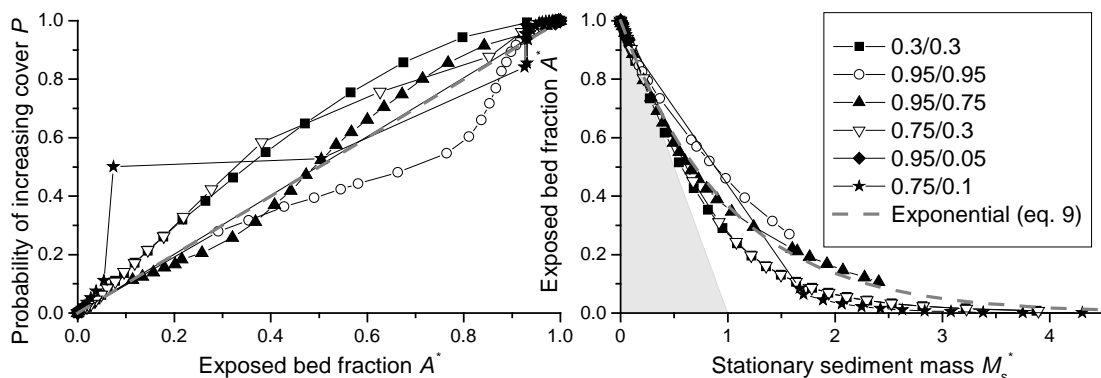
517

518 Model runs were completed with a six different combinations of p_i and p_c : 0.95/0.95, 0.95/0.75,
 519 0.75/0.10, 0.75/0.30, 0.30/0.30 and 0.95/0.05. These combinations were selected to cover the range
 520 of relationships between relative sediment supply Q_s^* and the exposed bed fraction A^* observed by
 521 Hodge and Hoey (2012). For each pair of p_i and p_c model runs were completed at least 20 different
 522 values of Q_s^* in order to quantify the model behaviour.

523

524 Cover bed fraction and total mass on the bed ~~produced given out~~ by the model were converted using
 525 eq. (3) into the ~~new~~ probabilistic framework (Fig. 34). The derivative was approximated by simple
 526 linear finite differences, which, in the case of run-away alluviation, resulted in a non-continuous
 527 curve due to large gradients. The exponential benchmark (eq. 98) is also shown for comparison. The
 528 different model parameterisations produce results in which the probability of deposition on bedrock
 529 is both more and less likely than in the baseline case, with some runs showing both behaviours. Cases
 530 where the probability is more than the baseline case (i.e. grains are more likely to fall on uncovered
 531 areas) are associated with runs in which grains in clusters are relatively immobile. These runs are
 532 likely to be particularly affected by the smoothing algorithm that acts to move sediment from
 533 alluviated to bedrock areas. All model parameterisations predict greater bed exposure for a given
 534 normalised mass than is predicted by a linear cover relationship (Figure 3b). Runs with relatively
 535 more immobile cluster grains have a lower exposed fraction for the same normalised mass. Runs
 536 with low values of p_i and p_c seem to lead to behavior in which cover is more likely than in the
 537 exponential benchmark, while for high values, it is less likely. However, ~~these~~ are complex
 538 interactions and ~~it is difficult to generalize the model behavior~~ ~~general statements cannot be made~~
 539 ~~straightforwardly~~.

540



541

542 Fig. 34: Probability functions P and cover function derived from data obtained from the model of
 543 Hodge and Hoey (2012). The grey dashed line shows the exponential benchmark behavior. Grey
 544 shading depicts the area where the cover function cannot run due to conservation of mass. The
 545 legend gives values of the probabilities of entrainment p_i and p_c used for the runs (see text).

546

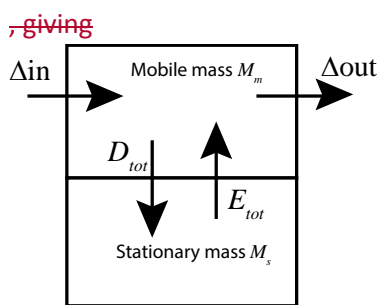
547

548 3. Cover development in time and space

549

550 3.1. Model derivation

551
552 Previous descriptions of the cover effect relate the exposed fraction of the bed to the relative
553 sediment supply Q_s^* (see eqs. 1 and 2). ~~The relation between Q_s^* and M_s , which we used in eq. (3),~~
554 ~~has often been muddled and incorrect (see, for example, Turowski et al., 2007).~~ In this
555 ~~chapter section,~~ we derive a model to clarify ~~this the relationship between the exposed fraction, Q_s^*~~
556 ~~and M_s relationship~~ and put it on a sound physical ~~basesbasis~~. To this end, the probabilistic
557 formulation introduced ~~previously above~~ is extended to allow the calculation of the temporal and
558 spatial evolution of sediment cover in a stream. Here, we will derive the equations for the one
559 dimensional case (linear flume), but extensions to higher dimensions are possible in principle. The
560 derivation is inspired by the erosion-deposition framework (e.g. Charru et al., 2004; ~~Turowski, 2009~~),
561 with some necessary adaptations to make it suitable for channels with partial sediment cover (~~e.g.,~~
562 ~~Turowski, 2009~~). In our system, we consider two separate mass reservoirs within a control volume.
563 The first reservoir contains all particles in motion, the total mass per bed area of which is denoted by
564 M_m , while the second reservoir contains all particles that are stationary on the bed, the total mass
565 per bed area of which is denoted by M_s . ~~The reservoirs can exchange mass by entrainment and~~
566 ~~deposition, i.e., when a stationary particle is entrained it becomes mobile and when a mobile particle~~
567 ~~is deposited, it becomes stationary. In addition to eq. 3, w~~We need then three further equations, one
568 to connect the rate of change of mobile mass to the sediment flux in the flume, ~~and one each to~~
569 ~~govern the exchange of particles between~~ describe mass conservation in the two reservoirs, ~~and one~~
570 ~~to describe how sediment transport rate is related to the mobile mass. The first of these is of course~~
571 ~~the Exner equation of sediment continuity (e.g. Paola and Voller, 2005), which captures mass~~
572 ~~conservation in the system.~~ Instead of the common approach tracking the height of the sediment
573 over a reference level, ~~as is done in the classic mass conservation in fluvial systems, the Exner~~
574 ~~equation (e.g. Paola and Voller, 2005),~~ we use the total sediment mass on the bed as a variable.
575 ~~Mobile sediment mass is supplied from upstream (Δin), leaves in the downstream direction (Δout)~~
576 ~~and can be exchanged between the stationary and the mobile mass reservoirs by entrainment (E_{tot})~~
577 ~~and deposition (D_{tot}) (Fig. 5). The latter two terms~~parameters describe the exchange of particles
578 ~~between reservoirs; in the single reservoir Exner equation these terms are not needed. It is clear that~~
579 ~~for the problem at hand the choice of total mass or volume as a variable to track the amount of~~
580 ~~sediment in the reach of interest is preferable to the height of the alluvial cover, since necessarily,~~
581 ~~when cover is patchy, the height of the alluvium varies across the bed.~~



583
584 Fig. 5: Sediment dynamics at the bed are modelled by two reservoirs for stationary and mobile mass,
585 which can exchange material by entrainment (E_{tot}) and deposition (D_{tot}). Sediment mass can be
586 supplied from upstream (Δin) and can leave into the downstream direction (Δout).

587
588 The difference form of the mass balance for the mobile sediment is then given by (cf. Fig. 5)

$$\Delta M_m = (\Delta in - \Delta out + E_{tot} - D_{tot})\Delta t$$

589
590 (eq. 12)

591 Here, ΔM_m is the change in mobile sediment mass and Δt is a change in time. As the length of a time
592 step is reduced to zero, a continuous version of eq. (12) is obtained, which reads

593

594

$$\frac{\partial M_m}{\partial t} = -\frac{\partial q_s}{\partial x} + E - D$$

595 (eq. 13)

596 Here, x is the coordinate in the streamwise direction, t the time, q_s the sediment mass transport rate
 597 per unit width, while E is the mass entrainment rate per bed area and D is the mass deposition rate
 598 per bed area. Similarly, in the mass balance for the stationary mass reservoir, the rate of change of
 599 the stationary sediment mass M_s in time is the difference of the deposition rate D and the
 600 entrainment rate E :

601

602

$$\frac{\partial M_s}{\partial t} = D - E$$

603 (eq. 16)

604 ~~The latter two terms describe the exchange of particles between reservoirs; in the single reservoir~~
 605 ~~Exner equation these terms are not needed. It is clear that for the problem at hand the choice of~~
 606 ~~total mass or volume as a variable to track the amount of sediment in the reach of interest is~~
 607 ~~preferable to the height of the alluvial cover, since necessarily, when cover is patchy, the height of~~
 608 ~~the alluvium varies across the bed.~~ It is useful to work with dimensionless variables by defining
 609 $t^* = t/T$ and $x^* = x/L$, where T and L are suitable time and length scales, respectively. The
 610 dimensionless mobile mass per bed area M_m^* is equal to M_m/M_0 , and eq. (13) becomes:

611

612

$$\frac{\partial M_m^*}{\partial t^*} = -\frac{\partial q_s^*}{\partial x^*} + E^* - D^*$$

613 (eq. 14)

614 Here,

615

$$q_s^* = \frac{T}{LM_0} q_s$$

616 (eq. 15)

617 The dimensionless entrainment and deposition rates, E^* and D^* , are equal to TE/M_0 and TD/M_0 ,
 618 respectively. ~~The rate of change of the stationary sediment mass M_s in time is the difference of the~~
 619 ~~deposition rate D and the entrainment rate E :~~

620

621

$$\frac{\partial M_s}{\partial t} = D - E$$

622 (eq. 16)

623 ~~Or~~ Similarly, using dimensionless variables the balance for the stationary mass (eq. 14) can be written
 624 as

625

626

$$\frac{\partial M_s^*}{\partial t^*} = D^* - E^*$$

627 (eq. 17)

628 We also need sediment entrainment and deposition functions. The entrainment rate needs to be
 629 modulated by the availability of sediment on the bed. If M_s^* is equal to zero, no material can be
 630 entrained. A plausible assumption is that the maximal entrainment rate, E_{max}^* , is equal to the
 631 transport capacity.

632

$$E_{max}^* = q_t^*$$

633 (eq. 18)

634 Here, q_t^* is the dimensionless mass transport capacity, which is related to the transport capacity per
 635 unit width q_t by a relation similar to eq. (15). To first order, the rate of change in entrainment rate,
 636 dE , is proportional to the difference of E_{max} and E , and to the rate of change in mass on the bed.

637

638

$$dE^* = (E_{max}^* - E^*)dM_s^* = (q_t^* - E^*)dM_s^*$$

639 (eq. 19)

640 Integrating, we obtain

641

642

$$E^* = E_{max}^*(1 - e^{-M_s^*}) = (1 - e^{-M_s^*})q_t^*$$

643 (eq. 20)

644 Here, we used the condition $E^*(M_s^*=0) = 0$ to fix the integration constant to E_{max}^* . As required, eq.

645 (20) approaches E_{max}^* as M_s^* goes to infinity, and is equal to zero when M_s^* is equal to zero. Using a

646 similar line of argument, and by assuming the maximum deposition rate to be equal to q_s^* , we arrive

647 at an equation for the deposition rate D^* .

648

649

$$D^* = (1 - e^{-M_m^*})q_s^*$$

650 (eq. 21)

651 When M_m^* is small, then the amount that can be deposited is limited by M_m^* . If M_m^* is large, then

652 deposition is limited by sediment supply. Substituting eqs. (20) and (21) into eq. (17), we obtain:

653

$$\frac{\partial M_s^*(x^*, t^*)}{\partial t^*} = D^* - E^* = (1 - e^{-M_m^*(x^*, t^*)})q_s^*(x^*, t^*) - (1 - e^{-M_s^*(x^*, t^*)})q_t^*(x^*, t^*)$$

654 (eq. 22)

655 Note that $q_s^*/q_t^* = Q_s^*$. The equation for the mobile mass (eq. 14) becomes:

656

$$\frac{\partial M_m^*(x^*, t^*)}{\partial t^*} = -\frac{\partial q_s^*}{\partial x^*} - (1 - e^{-M_m^*(x^*, t^*)})q_s^*(x^*, t^*) + (1 - e^{-M_s^*(x^*, t^*)})q_t^*(x^*, t^*)$$

657 (eq. 23)

658 Finally, the sediment transport rate needs to be proportional to the mobile sediment mass times the

659 downstream sediment speed U , and we can write

660

661

$$q_s^*(x^*, t^*) = U^*(x^*, t^*)M_m^*(x^*, t^*)$$

662 (eq. 24)

663 Here

664

$$U^* = \frac{T}{L}U$$

665 (eq. 25)

666

667 After incorporating the original equation between A^* and M_s^* (eq. 3), the system of four differential

668 equations (3), (22), (23) and (24) contains four unknowns: the downstream gradient in the sediment

669 transport rate $\partial q_s^*/\partial x^*$, the exposed fraction of the bed A^* , the non-dimensional stationary mass M_s^* ,

670 and the non-dimensional mobile mass M_m^* , while the non-dimensional transport capacity q_t^* and the

671 non-dimensional downstream sediment speed U^* are input variables, and P is an externally specified

672 function. In addition, sediment input q_s^* needs to be specified as an upstream boundary condition

673 and initial values for the mobile mass M_m^* and the stationary mass M_s^* need to be specified

674 everywhere.

675

676 3.2. Time-independent solution

677

678 In this chapter, we discuss the steady solution to the system of equations and thus clarify the

679 relationship between cover, stationary sediment mass, sediment supply and transport capacity.

680 Setting the time derivatives to zero, we obtain a time-independent solution, which links the exposed

683 area directly to the ratio of sediment transport rate to transport capacity. From eq. (23) it follows
 684 that in this case, the entrainment rate is equal to the deposition rate and we obtain

$$(1 - e^{-\bar{M}_m^*}) \bar{q}_s^* = (1 - e^{-\bar{M}_s^*}) q_t^*$$

685 (eq. 26)

687 Here, the bar over the variables denotes their steady state value. Substituting eq. (24) to eliminate
 688 \bar{M}_m^* and solving for \bar{M}_s^* gives

$$\bar{M}_s^* = -\ln \left\{ 1 - \left(1 - e^{-\bar{q}_s^*/U^*} \right) \frac{\bar{q}_s^*}{q_t^*} \right\} = -\ln \left\{ 1 - \left(1 - e^{-\frac{q_t^* \bar{Q}_s^*}{U^*}} \right) \bar{Q}_s^* \right\}$$

691 (eq. 27)

692 Note that we assume here that sediment cover is only dependent on the stationary sediment mass
 693 on the bed and we thus neglect grain-grain interactions known as the dynamic cover (Turowski et al.,
 694 2007). In analogy to eq. (24), we can write

$$q_t^* = U^* M_0^*$$

695 (eq. 28)

697 Here, M_0^* is a characteristic dimensionless mass that depends on hydraulics and therefore implicitly
 698 on transport capacity (which is independent of and should not be confused with the minimum mass
 699 necessary to fully cover the bed M_0). When sediment transport rate equals transport capacity, then
 700 M_0^* is equal to the mobile mass of sediment normalized by the reference mass M_0 . It can be viewed
 701 as a proxy for the transport capacity and is a convenient parameter to simplify the equations. The
 702 mobile mass can then, in general, be written as follows (cf. Turowski et al., 2007), remembering that
 703 the relative sediment supply $Q_s^* = 1$ when supply is equal to capacity:

$$M_m^* = M_0^* Q_s^*$$

705 (eq. 29)

706 If we use the exponential cover function (eq. 98) with eqs. (27), (28) and (29), we obtain

$$\bar{A}^* = 1 - \left(1 - e^{-\bar{q}_s^*/U^*} \right) \frac{\bar{q}_s^*}{q_t^*} = 1 - \left(1 - e^{-\frac{q_t^* \bar{Q}_s^*}{U^*}} \right) \bar{Q}_s^* = 1 - \left(1 - e^{-M_0^* \bar{Q}_s^*} \right) \bar{Q}_s^*$$

709 (eq. 30)

710 Similarly, equations can be found for the other analytical solutions of the cover function. For the
 711 linear case (eq. 76), we obtain:

$$\bar{A}^* = 1 + \ln \left\{ 1 - \left(1 - e^{-M_0^* \bar{Q}_s^*} \right) \bar{Q}_s^* \right\}$$

713 (eq. 31)

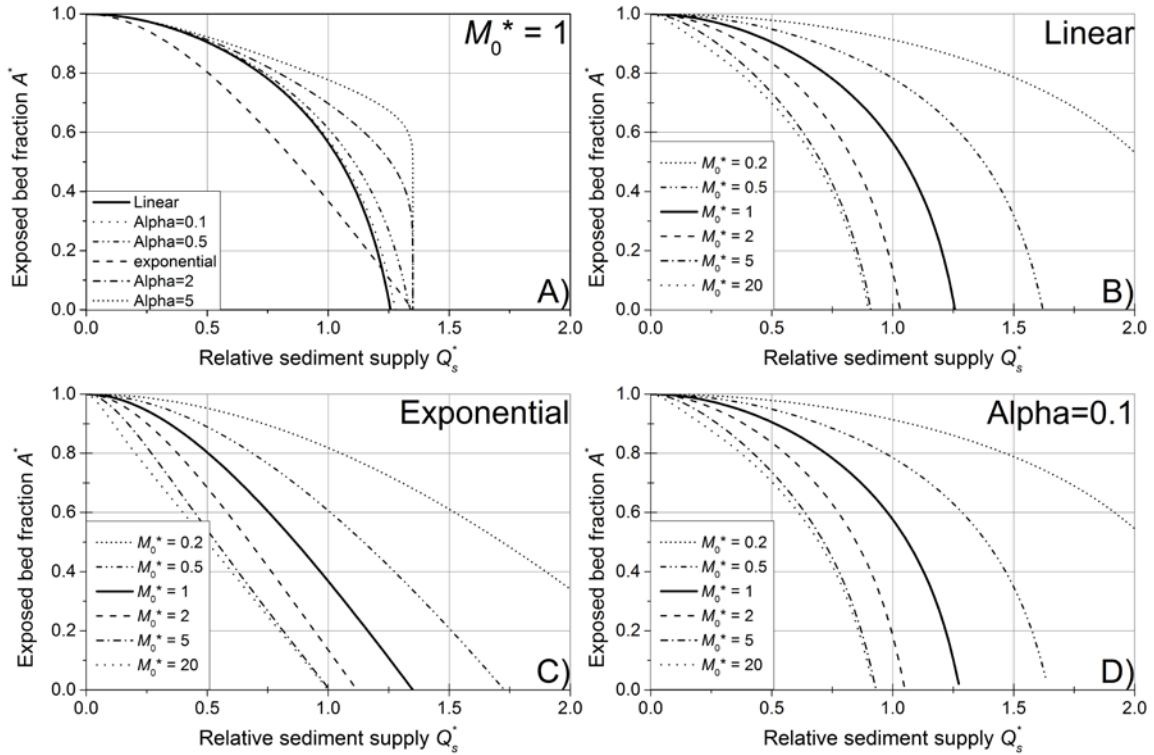
714 For the power law case (eq. 109), we obtain:

$$\bar{A}^* = \left[1 + (1 - \alpha) \ln \left\{ 1 - \left(1 - e^{-M_0^* \bar{Q}_s^*} \right) \bar{Q}_s^* \right\} \right]^{\frac{1}{1-\alpha}}$$

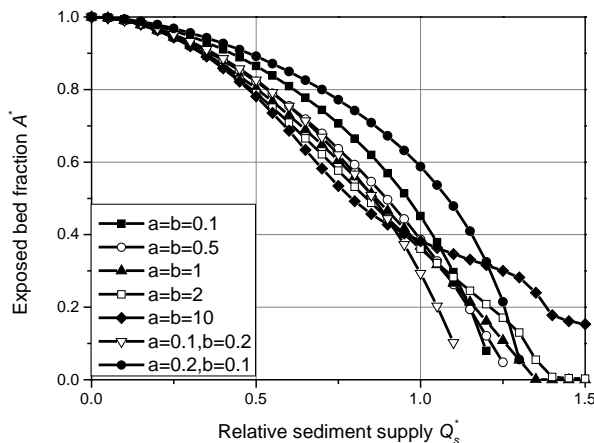
716 (eq. 32)

717 It is interesting that the assumption of an exponential cover function essentially leads to a
 718 combined linear and exponential relation between \bar{A}^* and \bar{Q}_s^* . Instead of a linear decline as the
 719 original linear cover model (eq. 1), or a concave-up relationship as the original exponential model
 720 (eq. 2), the function is convex-up for all solutions (Fig. 46). Adjusting M_0^* shifts the lines: decreasing
 721 M_0^* leads to a delayed onset of cover and vice versa. The former result arises because a lower M_0^*
 722 means that the sediment flux is conveyed through a smaller mass moving at a higher velocity. The
 723 original linear cover function (eq. 1) can be recovered from the exponential model with a high value
 724 of M_0^* , since the exponential term quickly becomes negligible with increasing \bar{Q}_s^* and the linear term
 725 dominates (Fig. 46C). Note that for the linear (eq. 65) and the power law cases (eq. 109), high
 726 values of M_0^* may give $\bar{A}^* = 0$ for $\bar{Q}_s^* < 1$ (Fig. 46B,D), which is consistent with the concept of

727 runaway alluviation. Using the beta distribution to describe P , a numerical solution is necessary, but
 728 a wide range of steady-state cover functions can be obtained (Fig. 57). By varying the value of M_0^* , an
 729 even wider range of behavior can be obtained.



730
 731 Fig. 46: Analytical solutions at steady state for the exposed fraction of the bed (A^*) as a function of
 732 relative sediment supply (Q_s^* , cf. Fig. 42). A) Comparison of the different solutions, keeping M_0^*
 733 constant at 1. B) Varying M_0^* for the linear case (eq. 31). C) Varying M_0^* for the exponential case (eq.
 734 30). D) Varying M_0^* for the power law case with $\alpha = 0.1$ (eq. 32).
 735



736
 737 Fig. 57: Steady state solutions using the beta distribution to parameterize P (eq. 4110) for a range of
 738 parameters a and b , and using $M_0^* = 1$ (cf. Fig. 23). The solutions were obtained by iterating the
 739 equations to a steady state, using initial conditions of $A^* = 1$ and $M_m^* = M_s^* = 0$.
 740

741 The previous analysis shows that steady state cover is controlled by the characteristic dimensionless
 742 mass M_0^* , which is equal to the ratio of dimensionless transport capacity and particle speed (eq. 28).
 743 In the following, we relate M_0^* to hydraulic variables and argue that it is, in general, not a constant.
 744 Converting M_0^* to dimensional variables, we can write

$$M_0^* = \frac{q_t^*}{U^*} = \frac{q_t}{M_0 U}$$

745 (eq. 33)

746 The minimum mass necessary to completely cover the bed per unit area, M_0 , can be estimated
 747 assuming a single layer of close-packed spherical grains residing on the bed (cf. Turowski, 2009),
 748 giving:

$$M_0 = \frac{\pi \rho_s D_{50}}{3\sqrt{3}}$$

750 (eq. 34)

751 Here, ρ_s is the sediment density and D_{50} is the median grain size. We use equations derived by
 752 Fernandez-Luque and van Beek (1976) from flume experiments that describe transport capacity and
 753 particle speed as a function of bed shear stress (see also Lajeunesse et al., 2010, and Meyer-Peter
 754 and Mueller, 1948, for similar equations):

$$q_t = 5.7 \frac{\rho_s \rho}{(\rho_s - \rho)g} \left(\frac{\tau}{\rho} - \frac{\tau_c}{\rho} \right)^{3/2}$$

755 (eq. 35)

$$U = 11.5 \left(\left(\frac{\tau}{\rho} \right)^{1/2} - 0.7 \left(\frac{\tau_c}{\rho} \right)^{1/2} \right)$$

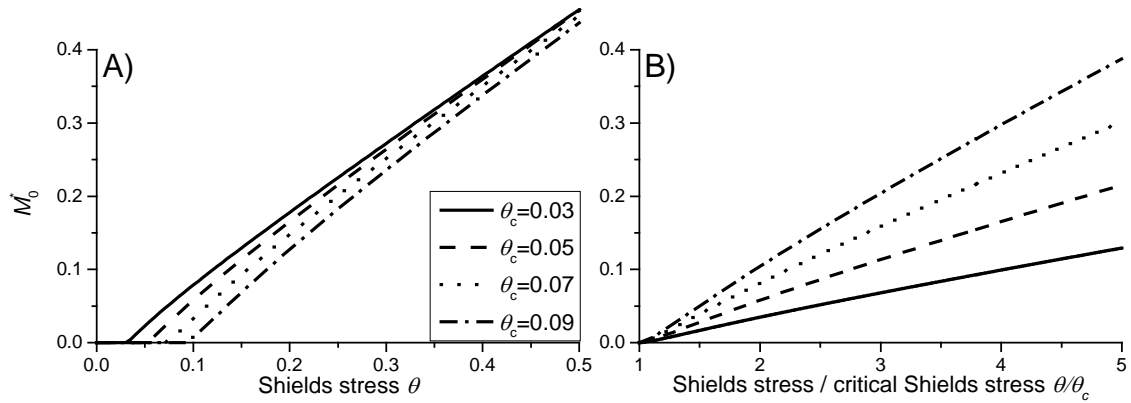
756 (eq. 36)

757 Here, τ_c is the critical bed shear stress for the onset of bedload motion, g is the acceleration due to
 758 gravity and ρ is the water density. Combining eqs. (34), (35) and (36) to get an equation for M_0^* gives:

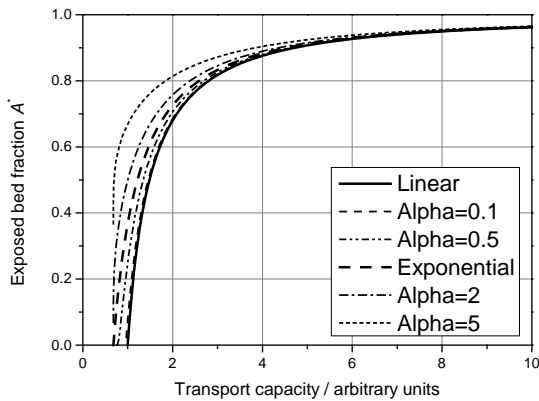
$$M_0^* = \frac{3\sqrt{3}}{2\pi} \frac{(\theta - \theta_c)^{3/2}}{\theta^{1/2} - 0.7\theta_c^{1/2}} = \frac{3\sqrt{3}\theta_c}{2\pi} \frac{(\theta/\theta_c - 1)^{3/2}}{(\theta/\theta_c)^{1/2} - 0.7}$$

760 (eq. 37)

761 Here, the Shields stress $\theta = \tau/(\rho_s - \rho)gD_{50}$, and θ_c is the corresponding critical Shields stress, and we
 762 approximated $5.7/11.5 = 0.496$ with $1/2$ (compare to eqs. 35/36). At high θ , when the threshold can
 763 be neglected, eq. (37) reduces to a linear relationship between M_0^* and θ . Near the threshold, M_0^* is
 764 shifted to lower values as θ_c increases (Fig. 68). The systematic variation of U^* with the hydraulic
 765 driving conditions (eq. 36) implies that the cover function evolves differently in response to changes
 766 in sediment supply and transport capacity. For a first impression, by comparing equations (35) and
 767 (36), we assume that particle speed scales with transport capacity raised to the power of one third
 768 (Fig. 79).



776
 777 Fig. 68: The characteristic dimensionless mass M_0^* depicted as a function of A) the Shields stress and
 778 B) the ratio of Shields stress to critical Shields stress (eq. 37).
 779



780
 781 Fig. 79: Variation of the exposed bed fraction as a function of transport capacity, assuming that
 782 particle speed scales with transport capacity to the power of one third.
 783

784 3.3 Temporal evolution of cover within a reach

785
 786 To calculate the temporal evolution of cover on the bed within a single reach, we solved equations
 787 (3), (22), (23) and (24) numerically for a section of the bed with homogenous conditions using a
 788 simple linear finite difference scheme. Then in this case, sediment input is a boundary condition,
 789 while sediment output, mobile and stationary sediment mass and the fraction of the exposed bed are
 790 output variables. In general, a change in sediment supply leads to a gradual adjustment of the output
 791 variables towards a new steady state (Fig. 10). It would be desirable to obtain expressions for the
 792 response time of the system to external perturbation, such as a change in sediment supply or
 793 hydraulic conditions. Such a response time could then be compared to the time scales of changes in
 794 boundary conditions. For example, during a flood event, both transport capacity and sediment supply
 795 change over time. If these changes are slow in comparison of the response time of cover, the bed
 796 cover state can essentially keep up with the imposed changes at all times and therefore steady state
 797 equations (section 3.2) can be used to calculate its evolution. In contrast, if the imposed change is
 798 rapid in comparison to the response time, cover may lag behind and an approach that resolves
 799 cover as a dynamic variable is necessary. This may, for example, be important when studying the
 800 erosional behavior of channels in response to floods (see Lague, 2010; Turowski et al., 2013).
 801 Unfortunately, a general analytical solution is not possible, but results can be obtained for special
 802 cases. We first derive analytical solutions for the response time for a reach without upstream
 803 sediment supply and for a system responding to small perturbations in sediment supply or transport

capacity (section 3.3.1) and discuss the system behavior in the latter case (section 3.3.2). Finally, we apply the concepts to data from a flood in a natural river and demonstrate that, for this specific case, because of the response times the steady state relations do not capture cover behavior.

3.3.1 System timescales

To calculate the temporal evolution of cover on the bed within a single reach, we solved the equations numerically for a section of the bed with homogenous conditions using a simple linear finite difference scheme. Then, the sediment input is a boundary condition, while sediment output, mobile and stationary sediment mass and the fraction of the exposed bed are output variables. In general, a change in sediment supply leads to a gradual adjustment of the output variables towards a new steady state (Fig. 8). Unfortunately, a general analytical solution is not possible, but a result can be obtained for the special case. First, consider a reach without upstream sediment supply, i.e., of $q_s^* = 0$. Such a situation is rare in nature, but could be easily created in flume experiments as a model test. Then, the time derivative of stationary mass is given by:

$$\frac{\partial M_s^*}{\partial t^*} = -(1 - e^{-M_s^*})q_t^*$$

(eq. 38)

Using the exponential cover model (eq. 98), we obtain:

$$\frac{1}{A^*(1 - A^*)} \frac{\partial A^*}{\partial t^*} = q_t^*$$

(eq. 39)

Equation (39) is separable and can be integrated to obtain

$$\ln(A^*) - \ln(1 - A^*) = t^*q_t^* + C$$

(eq. 40)

Letting $A^*(t^*=0) = A_0^*$, where A_0^* is the initial cover, the final equation is

$$\frac{1 - A^* A_0^*}{1 - A_0^* A^*} = e^{-t^*q_t^*}$$

(eq. 41)

To clarify the characteristic time scale of the process, equation (41) can also be written in the form of a sigmoidal-type function:

$$A^* = \frac{1}{1 + \left(\frac{1 - A_0^*}{A_0^*}\right) e^{-t^*q_t^*}}$$

(eq. 42)

By making the parameters in the exponent on the right hand side of eq. (42) dimensional, we get:

$$t^*q_t^* = \frac{t}{T} \frac{T}{LM_0} q_t = \frac{tq_t}{LM_0}$$

(eq. 43)

which allows a characteristic system time scale T_E to be defined as

$$T_E = \frac{LM_0}{q_t}$$

(eq. 44)

845 Since this time scale is dependent on the transport capacity q_t , we can view it as a time scale
 846 associated with the entrainment of sediment from the bed (cf. eq. 20) – hence the subscript E on T_E .
 847 From eq. (4241), the exposed bed fraction evolves in an asymptotic fashion towards equilibrium
 848 (Fig. 911). We can expect that there are other characteristic time scales for the system, for example
 849 associated with sediment deposition or downstream sediment evacuation.

850

851 We can make some further progress and define a more general system time scale by performing a
 852 perturbation analysis (Appendix A). For small perturbations in either q_s^* or q_t^* , we obtain an
 853 exponential term describing the transient evolution, which allows the definition of a system
 854 timescale T_S

$$855 \quad \exp \left\{ - \left(\bar{q}_t^* - \left(1 - e^{-\bar{q}_s^*/\bar{U}^*} \right) \bar{q}_s^* \right) t^* \right\} = e^{-\frac{t}{T_S}} \exp \left\{ -\frac{t}{T_S} \right\}$$

856 (eq. 4544)

857 Here, exp denotes the natural exponential function. The characteristic system time scale can then be
 858 written as

$$859 \quad T_S = \frac{LM_0}{\bar{q}_t \left(1 - \left(1 - e^{-\bar{q}_s^*/\bar{U}^*} \right) \frac{\bar{q}_s}{\bar{q}_t} \right)} = \frac{LM_0}{\bar{q}_t} e^{\bar{M}_s^*}$$

860 (eq. 4645)

861 Note that for $q_s^* = 0$, eq. (4645) reduces to eq. (4443), as would be expected. Since \bar{M}_s^* is directly
 862 related to steady state bed exposure \bar{A}^* , we can rewrite the equation, for example by assuming the
 863 exponential cover function (eq. 38), as

$$864 \quad T_S = \frac{LM_0}{\bar{q}_t \bar{A}^*}$$

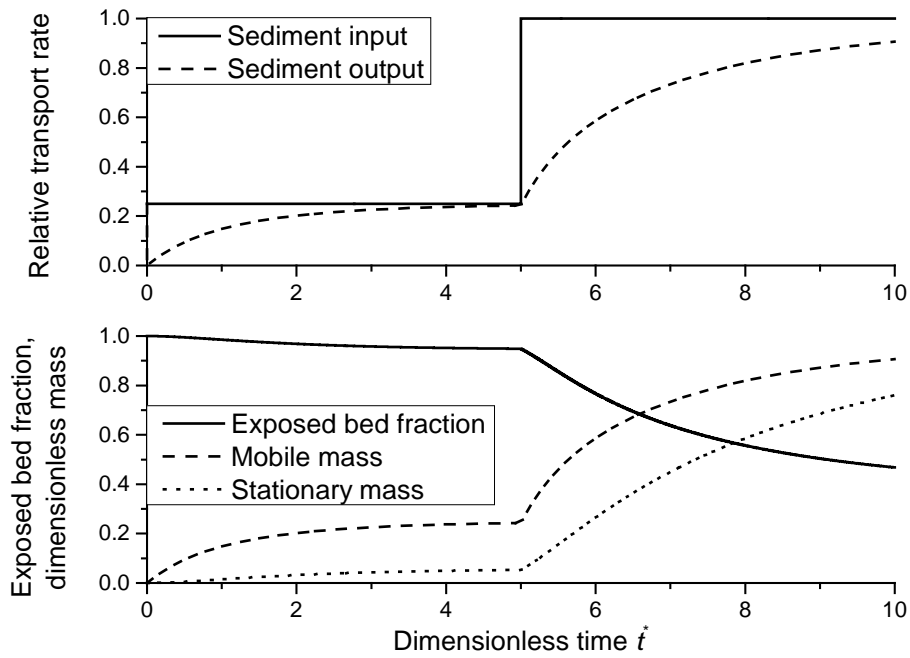
865 (eq. 4746)

866 Since bed cover is more easily measurable than the mass on the bed, eq. (4746) can help to estimate
 867 system time scales in the field. Further, \bar{A}^* varies between 0 and 1, which allows [the estimation of](#)
 868 [a minimum system time using eq. \(4443\)](#). As \bar{A}^* approaches zero, the system time scale diverges.

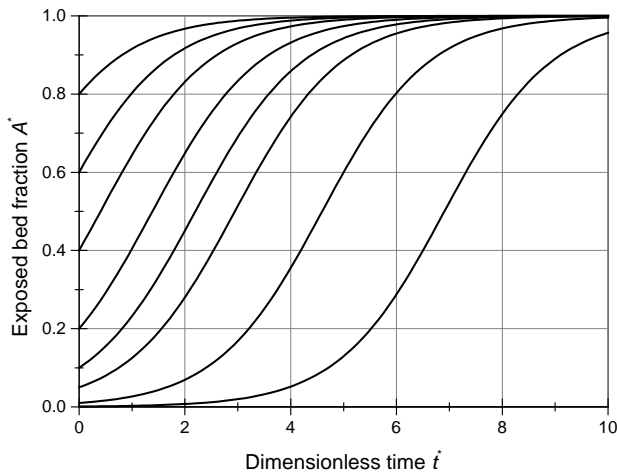
869

870 To illustrate these additional dependencies, we have used numerical solutions of eqs. (3), (22), (23)
 871 and (24) to calculate the time needed to reach 99.9% of total adjustment after a step change in
 872 transport stage (chosen due to the asymptotic behavior of the system), [analysed across a plausible](#)
 873 [range of produced by varying particle speeds \$U\$ over a range of plausible values](#) (Fig. 1012). Response
 874 time decreases as particle speed increases. This reflects elevated downstream evacuation for higher
 875 particles speeds, resulting in a smaller mobile particle mass and thus higher entrainment and lower
 876 deposition rates. Response time also increases with increasing relative sediment supply Q_s^* . As the
 877 runs start with zero sediment cover, and the extent of cover increases with Q_s^* , at higher Q_s^* the
 878 adjusted cover takes longer to develop.

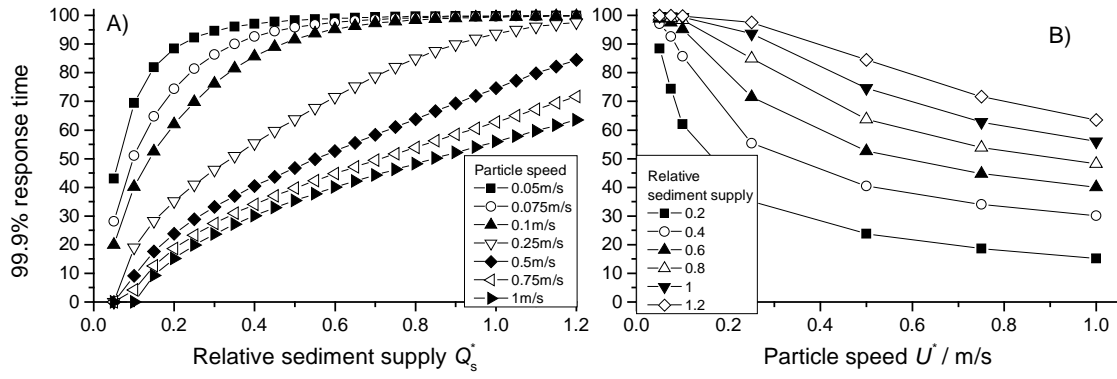
879



880
 881 Fig. 810: Temporal evolution of cover for the simple case of a control box with sediment through-
 882 flux, based on eqs. (3), (22), (23) and (24). Relative sediment supply (supply normalized by transport
 883 capacity) was specified to 0.25 and increased to 1 at $t^* = 5$. The response of sediment output, mobile
 884 and stationary sediment mass and the exposed bed fraction was calculated. Here, we used the
 885 exponential function for P (eq. 98) and $M_0^* = U^* = 1$. The initial values were $A^* = 1$ and $M_m^* = M_s^* = 0$.
 886



887
 888 Fig. 911: Evolution of the exposed bed fraction (removal of sediment cover) over time starting with
 889 different initial values of bed exposure, for the special case of no sediment supply, i.e., $q_s^* = 0$ (eq. 41)
 890 and $q_t^* = 1$.
 891



892
893 Fig. 1012: Dimensionless time to reach 99.9% of the total adjustment in exposed area as a function of
894 A) transport stage and B) particle speed. All simulation were started with $A^* = 1$ and $M_m^* = M_s^* = 0$.
895
896

897 3.3.2 Phase shift and gain in response to a cyclic perturbation

898 The perturbation analysis (Appendix A) gives some insight into the response of cover to cyclic
899 sinusoidal perturbations. Let sediment supply be perturbed in a cyclic way described by an equation
900 of the form

$$901 \quad q_s^* = \overline{q_s^*} + \delta q_s^* = \overline{q_s^*} + d \sin\left(\frac{2\pi t}{p}\right)$$

902 (eq. 4847)

903 Here, the overbar denotes the temporal average, δq_s^* is the time-dependent perturbation, d is the
904 amplitude of the perturbation and p its period. A similar perturbation can be applied to the transport
905 capacity (see Appendix A). The reaction of the stationary mass and therefore cover can then also be
906 described by sinusoidal function of the form (Appendix A)

$$907 \quad \delta M_s^* = G \sin\left(\frac{2\pi t}{p} + \varphi\right)$$

908 (eq. 4948)

909 Here, δM_s^* is the perturbation of the stationary sediment mass around the temporal average, G is
910 known as the gain, describing the amplitude response, and φ is the phase shift. If the gain is large,
911 stationary mass reacts strongly to the perturbation; if it is small, the forcing does not leave a signal.
912 The phase shift is negative if the response lags behind the forcing and positive if it leads. The phase
913 shift can be written as

$$914 \quad \varphi = \tan^{-1}\left(-2\pi \frac{T_s}{p}\right)$$

915 (eq. 5049)

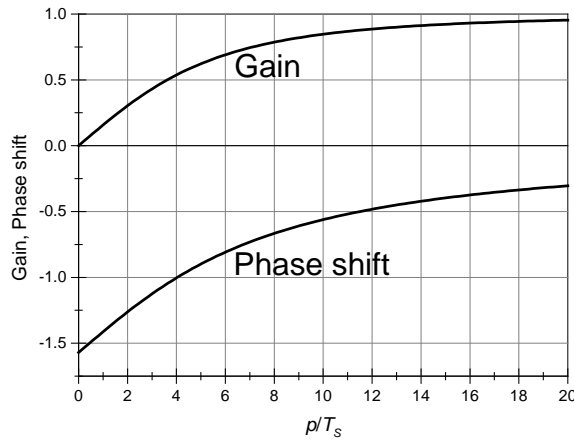
916 The gain can be written as

$$917 \quad G = \frac{p}{T_s} \frac{Kd}{\sqrt{\left(\frac{p}{T_s}\right)^2 + 4\pi^2}}$$

918 (eq. 5150)

919 Here, d is the amplitude of the perturbation, and K is a function of the time-averaged values of q_s , q_i
920 and U and differs for perturbations in transport capacity and sediment supply (see Appendix A).
921 Thus, the system behavior can be interpreted as a function of the ratio of the period of perturbation
922 p and the system time scale T_s . The period p is large if the forcing parameter, i.e., discharge or
923 sediment supply, varies slowly and small when it varies quickly. According to eq. (5049), the phase
924 shift is equal to $-\pi/2$ for low values of p/T_s (quickly-varying forcing parameter), implying a substantial
925 lag in the adjustment of cover. The phase shift tends to zero as p/T_s tends to infinity (Fig. 1113). The

926 gain varies approximately linearly with p/T_s for small p/T_s (quickly-varying forcing parameter), while it
 927 is approximately constant at a value of Kd for large p/T_s (slowly-varying forcing parameter) (eq.
 928 [5150](#)). Thus, if the forcing parameter varies slowly, cover adjustment keeps up at all times.
 929



930
 931 Fig. [1113](#): Phase shift (eq. [5049](#)) and gain (eq. [5150](#)) as a function of the ratio of the period of
 932 perturbation p and the system time scale T_s . For the calculation, the constant factor in the gain (Kd)
 933 was set equal to one.
 934

935 3.3.3 A flood at the Erlenbach

936 To illustrate the magnitude of the timescales using real data, we use a flood dataset from the
 937 Erlenbach, a sediment transport observatory in the Swiss Prealps (e.g., Beer et al., 2015). There, near
 938 a discharge gauge, bedload transport rates are measured at 1-minute resolution using the Swiss Plate
 939 Geophone System, a highly developed and fully calibrated surrogate bedload measuring system (e.g.,
 940 Rickenmann et al., 2012; Wyss et al. 2016). We use data from a flood on 20th June 2007 (Turowski et
 941 al., 2009) with highest peak discharge that has so far been observed at the Erlenbach. The
 942 meteorological conditions that triggered this flood and its geomorphic effects have been described in
 943 detail elsewhere (Molnar et al., 2010; Turowski et al., 2009, 2013). The Erlenbach does not have a
 944 bedrock bed in the sense that bedrock is exposed in the channel bed, however, the data provide a
 945 realistic natural time series of discharge and bedload transport over the course of a single event.
 946 Rather than predicting bed cover evolution for a natural system, for which we do not currently have
 947 data for validation, we use the Erlenbach data to illustrate possible cover behavior during a fictitious
 948 event with different initial sediment cover extents, using natural data to provide realistic boundary
 949 conditions.
 950

951 Using a median grain size of 80 mm, a sediment density of 2650 kg/m³ and a reach length of 50 m,
 952 we obtained $M_0 = 128 \text{ kg/m}^2$. We calculated transport capacity using the equation of Fernandez
 953 Luque and van Beek (1976). However, it is known that this and similar equations strongly
 954 overestimate measured transport rates in streams such as the Erlenbach (e.g., Nitsche et al., 2011).
 955 Consequently, we rescaled by setting the ratio of bedload supply to capacity to one at the highest
 956 discharge. The exposed fraction was then calculated iteratively assuming $P = A^*$ (i.e., the exponential
 957 cover formulation, eq. [98](#)). In a real flood event, water discharge and sediment supply obviously do
 958 not follow a small cyclic perturbation (Fig. [1113](#)). But we can tentatively relate the observations to
 959 the theory by assuming that at each time step, the change in sediment supply can be represented by
 960 the commencement of a sinusoidal perturbation with varying period. To estimate the effective
 961 period p , one needs to take the derivatives of eq. [\(4847\)](#).

962

$$\frac{dq_s^*}{dt} = \frac{d\delta q_s^*}{dt} = \frac{2\pi d}{p} \cos\left(\frac{2\pi t}{p}\right)$$

963 (eq. 5251)

964 Setting $t = 0$ for the time of interest, we can relate p to the local gradient in bedload supply, which
 965 can be measured from the data.

966

$$\frac{2\pi d}{p} = \frac{\Delta q_s^*}{\Delta t}$$

967

968 (eq. 52)

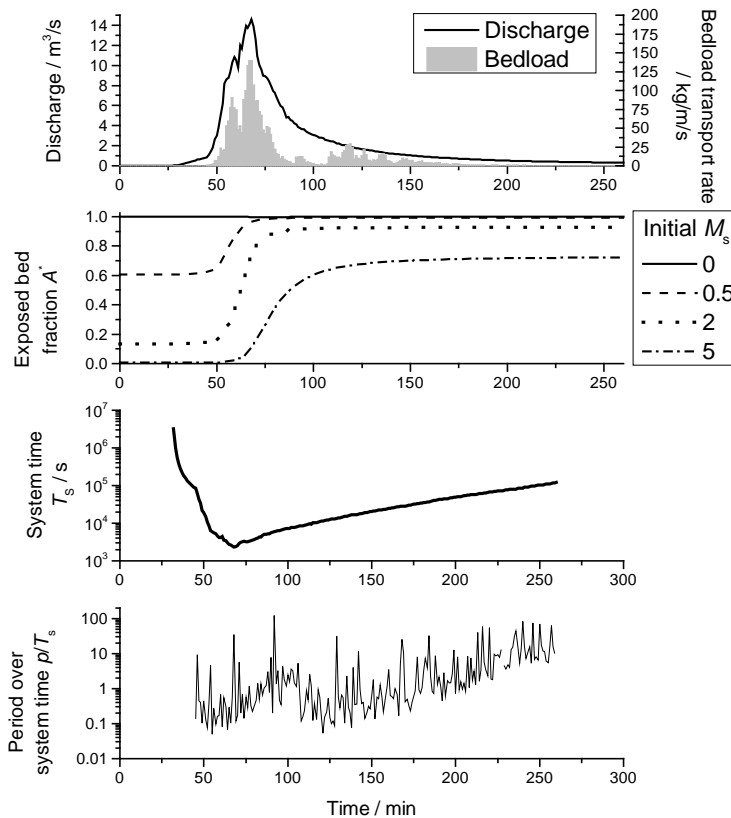
969 Assuming that all change in the response time is due to changes in the period (i.e., assuming a
 970 constant amplitude, $d = 1$), we can obtain a conservative estimate of the range over which p varies
 971 over the course of an event.

972

$$p = 2\pi \frac{\Delta t}{\Delta q_s^*}$$

973 (eq. 5253)

974 In the exemplary event, the evolution and final value of bed cover depends strongly on its initial
 975 value (Fig. 1214), indicating that the adjustment is incomplete. The system timescale is generally
 976 larger than 1000_s and is inversely related to discharge via the dependence on transport capacity.
 977 The p/T_s ratio varies around one, with low values at the beginning of the flood and large values in the
 978 waning hydrograph. Both the high values of the system time scale and the smooth evolution of bed
 979 cover over the course of the flood imply that cover development cannot keep up with the variation in
 980 the forcing characteristics. This dynamic adjustment of cover, which can lag forcing processes, may
 981 thus play an important role in the dynamics of bedrock channels and probably needs to be taken into
 982 account in modelling.



983

984 Fig. 1214: Calculated evolution of cover during the largest event observed at the Erlenbach on 20th
985 June 2007 (Turowski et al., 2009). Bedload transport rates were measured with the Swiss Plate
986 geophone sensors calibrated with direct bedload samples (Rickenmann et al., 2012). The final
987 fraction of exposed bedrock is strongly dependent on its initial value.
988

989 4. Discussion

990 4.1 Model formulation

991 In principle, the framework for the cover effect presented here allows the formulation of a general
992 model for bedrock channel morphodynamics without the restrictions of previous models (e.g. Nelson
993 and Seminara, 2011; Zhang et al., 2015). To achieve this, the dependency of P on various control
994 parameters needs to be specified. In general, P should be controlled by local topography, grain size
995 and shape, hydraulic forcing, and the amount of sediment already residing on the bed. Furthermore,
996 the shape of the P function should also be affected by feedbacks between these properties, such as
997 the development of sediment cover altering the local roughness and hence altering hydraulics and
998 local transport capacity (Inoue et al., 2014; Johnson, 2014). Within the treatment presented here, we
999 have explicitly accounted only for the impact of the amount of sediment already residing on the bed.
1000 However, all of the mentioned effects can be included implicitly by an appropriate choice of P . The
1001 exact relationships between, say, bed topography and P need to be mapped out experimentally (e.g.,
1002 Inoue et al., 2014), with theoretical approaches also providing some direction (cf. Johnson, 2014;
1003 Zhang et al., 2015). Currently available experimental results (Chatanantavet and Parker, 2008;
1004 Finnegan et al., 2007; Hodge and Hoey, 2016; Inoue et al., 2014; Johnson and Whipple, 2007) cover
1005 only a small range of the possible parameter space and, in general, not all necessary parameters to
1006 constrain P were reported. Specifically the stationary mass of sediment residing on the bed is usually
1007 not reported and can be difficult to determine experimentally, but is necessary to determine P .
1008 Nevertheless, depending on the choice of P , our model can yield a wide range of cover functions that
1009 encompasses reported functions both from numerical modelling (e.g., Aubert et al., 2016; Hodge and
1010 Hoey, 2012; Johnson, 2014) and experiments (Chatanantavet and Parker, 2008; Inoue et al., 2014;
1011 Sklar and Dietrich, 2001) (see Figs. 4 and 5).
1012

1013 The dynamic model put forward here is a minimum first order formulation, and there are some
1014 obvious future alterations. We only take account of the static cover effect caused by immobile
1015 sediment on the bed. The dynamic cover effect, which arises when moving grains interact at high
1016 sediment concentration and thus reduce the number of impacts on the bed (Turowski et al., 2007),
1017 could in principle be included into the formulation, but would necessitate a second probability
1018 function specifically to describe this dynamic cover. It would also be possible to use different P -
1019 functions for entrainment and deposition, thus introducing hysteresis into cover development. Such
1020 hysteresis has been observed in experiments in which the equilibrium sediment cover was a function
1021 of the initial extent of sediment cover (Chatanantavet and Parker, 2008; Hodge and Hoey, 2012).
1022 Whether such alterations are necessary is best established with targeted laboratory experiments.
1023

1024 4.2 Comparison to previous modelling frameworks

1025 We will briefly outline in this section the main differences to previous formulations of cover dynamics
1026 in bedrock channels. Thus, the novel aspects of our formulation and the respective advantages and
1027 disadvantages will become clear.
1028

1029 Aubert et al. (2015) coupled the movement of spherical particles to the simulation of a turbulent
1030 fluid and investigated how cover ~~depended~~ depends on transport capacity and supply. Similar to
1031 what is predicted by our analytical formulation, they found a range of cover function for various

1032 model set-ups, including linear and convex-up relationships (compare the results in Fig. 4-6 to their
1033 Fig. 15). ~~Despite short-comings,~~ Aubert et al. (2015) presented the so far most detailed physical
1034 simulations of bed cover formation and the correspondence between the predictions is encouraging.

1035
1036 Nelson and Seminara (2011, ~~2011~~2012) formulated a morphodynamic model for bedrock channels.
1037 They based their formulation on sediment concentration, which is in principle similar to our
1038 formulation based on mass. However, Nelson and Seminara (2011, 2012) did not distinguish between
1039 mobile and stationary sediment and linked local transport directly to sediment concentration.

1040 ~~Further, Further, a given mass can be distributed in multiple ways to achieve various degrees of~~
1041 ~~cover, a fact that is quantified in our formulation by the probability parameter P .~~ Nelson and
1042 Seminara (2011, 2012) assumed a direct correspondence between sediment concentration and
1043 degree of cover, which is equivalent to the linear cover ~~assumption-function~~ (eq. 76),). ~~In this case, it~~
1044 ~~is assumed that grains are always deposited on uncovered bed and the different possible with the~~
1045 ~~associated problems outlined earlier distributions of particles within a grid node are not taken into~~
1046 ~~account.~~ Practically, this implies that the grid size needs to be of the order of the grain size, ~~because,~~
1047 ~~strictly, the assumption is only valid if a single grain can cover an entire grid node (cf. Fig. 1).~~

1048 Although different in various details, Inoue et al. (2016) have used essentially the same approach as
1049 Nelson and Seminar (2011, 2012) to link bedload concentration, transport and bed cover. Both of
1050 these models allow the 2D modelling of bedrock channel morphology. Although we have not fully
1051 developed such a model in the present paper, our model framework could easily be extended to 2D
1052 problems.

1053
1054 Inoue et al. (2014) formulated a 1D model for cover dynamics and bedrock erosion. There, they
1055 distinguish between stationary and mobile sediment using an Exner equation to capture sediment
1056 mass conservation. The degree of bed cover is related to transport rates and sediment mass via a
1057 saturation volume, which is related to our characteristic mass M_0^* (see section 3.2). A key difference
1058 between Inoue et al.'s (2014) model and the one presented here lies in the sediment ~~continuity-mass~~
1059 ~~conservation~~ equations (eqs. 2613 and 14), in which we explicitly take account of both entrainment
1060 and deposition. In addition, with the function P , describing the relationship between deposited mass
1061 and degree of cover, we provide a more flexible framework for complex simulations where the bed
1062 needs to be discretized (e.g., 2D models or reach-scale formulations).

1063
1064 Zhang et al. (2015) formulated a bed cover model specifically for beds with macro-roughness. There,
1065 deposited sediment always fills topographic lows from their deepest positions, such that there is a
1066 reach-uniform sediment level. While the model ~~is interesting and~~ provides a fundamentally different
1067 approach to what is suggested here, its applicability is limited to very rough beds and the assumption
1068 of a sediment elevation that is independent of the position on the bed seems physically unrealistic. In
1069 principle, the probabilistic framework presented here should be able to deal with macro-rough beds
1070 ~~as well, by making the P -function (eq. 3) explicitly dependent on roughness,~~ and thus allows a more
1071 general treatment of the problem of bed cover.

1072
1073 Within this paper, we focused on the dynamics of bed cover, rather than ~~on the~~ modelling of the
1074 dynamics of entire channels. The probabilistic formulation using the parameter P provides a flexible
1075 framework to connect the sediment mass residing on the bed with the exposed bedrock fraction.
1076 This particular element has not been treated in any of the previous models and could be easily
1077 implemented in other approaches dealing with sediment fluxes along and across the stream and the
1078 interaction with erosion and, over long time scales, channel morphology. However, it is as yet
1079 unclear how flow hydraulics, sediment properties and other conditions affect P and this should be

1080 investigated in targeted laboratory experiments. ~~Nevertheless, the proposed formulation provides a~~
1081 ~~framework in which data from various sources can be easily compared and discussed.~~

1082 1083 **4.3 Further implications**

1084 Based on field data interpretation, Phillips and Jerolmack (2016) argued that bedrock rivers adjust
1085 such that, similar to alluvial channels, medium sized floods are most effective in transporting
1086 sediment, and that channel geometry therefore can quickly adjust their transport capacity to the
1087 applied load and therefore achieve grade (cf. Mackin, 1948). They conclude that bedrock channels
1088 can adjust their morphologic parameters (channel width and shape) quickly in response to changing
1089 boundary conditions, ~~a somewhat counter-intuitive notion for slowly-eroding channels.~~ CIn contrast,
1090 our model suggests that instead bed cover can be adjusted to achieve grade. In steady state, time
1091 derivatives need to be equal to zero. Thus, entrainment equals deposition (eq. 1614), implying that
1092 the downstream gradient in sediment transport rate is equal to zero (eq. 1413). When sediment
1093 supply or transport capacity change, the exposed bedrock fraction can adjust to achieve a new
1094 steady state and a change of the channel geometry is unnecessary. These changes in sediment cover
1095 can occur far more rapidly than changes in width and cross-sectional shape (compare to eq. 4746).
1096 Whether a steady state is achieved depends on the relative magnitude of the timescales of
1097 perturbation and cover adjustment (see section 3.2). Our results imply that bedrock channels have
1098 two distinct time scales to adjust to changing boundary conditions to achieve grade. Over short
1099 times, bed cover is adjusted. This can occur rapidly. Over long time scales, channel width, cross-
1100 sectional shape and slope are adjusted.

1101 1102 **5. Conclusions**

1103
1104 The probabilistic view put forward in this paper offers a framework into which diverse data on bed
1105 cover, whether obtained from field studies, laboratory experiments or numerical modeling, can be
1106 easily converted to be meaningfully compared. The conversion requires knowledge of the mass of
1107 sediment on the bed and the evolution of exposed fraction of the bed. Within the framework,
1108 individual data sets can be compared to the exponential benchmark and linear limit cases, enabling
1109 physical interpretation. Furthermore, the formulation allows the general dynamic sub-grid modelling
1110 of bed cover. Depending on the choice of P , the model yields a wide range of possible cover
1111 functions. Which of these functions are appropriate for natural rivers and how they vary with factors
1112 including topography needs to be mapped out experimentally.

1113
1114 It needs to be noted here that the precise formulation of the entrainment and deposition functions
1115 also affects steady state cover relations. When calibrating P on data, it cannot always be decided
1116 whether a specific deviation from the benchmark case results from varying entrainment and
1117 deposition processes or from changes in the probability function driven for example by variations in
1118 roughness. For the prediction of the steady state cover relations and for the comparison of data sets,
1119 this should not matter, but the dynamic evolution of cover could be strongly affected.

1120
1121 The system timescale for cover adjustment is inversely related to transport capacity. This time scale
1122 can be long and in many realistic situations, cover cannot instantaneously adjust to changes in the
1123 forcing conditions. Thus, dynamic cover adjustment needs to be taken into account when modelling
1124 the long-term evolution of bedrock channels.

1125
1126 Our model formulation implies that bedrock channels adjust bed cover to achieve grade. Therefore,
1127 bedrock channel evolution is driven by two optimization principles. On short time scales, bed cover

1128 adjusts to match the sediment output of a reach to its input. Over long time scales, width and slope
1129 of the channel evolve to match long-term incision rate to tectonic uplift or base level lowering rates.
1130

1131 **Appendix A: Perturbation analysis**

1132

1133 Here, we derive the effect of a small sinusoidal perturbation of the driving variables, namely
 1134 sediment supply q_s^* and transport capacity q_t^* , on cover development. The perturbation of the
 1135 driving variables can be written as

$$1136 q_s^* = \bar{q}_s^* + \delta q_s^*$$

1137 (eq. A1)

$$1138 q_t^* = \bar{q}_t^* + \delta q_t^*$$

1139 (eq. A2)

1140 Here, the bar denotes the average of the quantity at steady state, while δq_s^* and δq_t^* denote the
 1141 small perturbation. The exposed area can be similarly written as

$$1142 A^* = \bar{A}^* + \delta A^*$$

1143 (eq. A3)

1144 Steady state cover is directly related to the mass on the bed M_s^* by eq. (3), which, as long as P is
 1145 independent of time, we can rewrite as

$$1146 \frac{dA^*}{dt} = -P \frac{dM_s^*}{dt}$$

1147 (eq. A4)

1148 Substituting eq. (A3) and a similar equation for M_s^* ,

$$1149 M_s^* = \bar{M}_s^* + \delta M_s^*$$

1150 (eq. A5)

1151 we obtain

$$1152 \frac{d\delta A^*}{dt} = -P \frac{d\delta M_s^*}{dt}$$

1153 (eq. A6)

1154 Here, the averaged terms drop out as they are independent of time. If P and the steady state
 1155 solution for A^* are known, a direct relationship between A^* and M_s^* can be derived. For example, for
 1156 the exponential cover model (eq. 28), substituting eqs. (A3) and (A5), we find

$$1157 \bar{A}^* + \delta A^* = e^{-\bar{M}_s^* - \delta M_s^*} = e^{-\bar{M}_s^*} e^{-\delta M_s^*} = \bar{A}^* e^{-\delta M_s^*} \approx \bar{A}^* (1 - \delta M_s^*)$$

1158 (eq. A7)

1159 Here, since the δ variables are small, we approximated the exponential term using a Taylor expansion
 1160 to first order. We obtain

$$1161 \delta A^* = -\bar{A}^* \delta M_s^*$$

1162 (eq. A8)

1163 It is therefore sufficient to derive the perturbation solution for M_s^* , the time evolution of which is
 1164 given by eq. (22). Eliminating M_m^* using eq. (24), we obtain

$$1165 \frac{\partial \delta M_s^*}{\partial t^*} = \left(1 - e^{-q_s^*/U^*}\right) q_s^* - \left(1 - e^{-M_s^*}\right) q_t^*$$

1166 (eq. A9)

1167

1168 **Perturbation of sediment supply**

1169

1170 First, let's look at a perturbation of sediment supply q_s^* , while other parameters are held constant.
 1171 Substituting eq. (A1) and (A5) into (A9), we obtain

$$1172 \frac{\partial \delta M_s^*}{\partial t^*} = \left(1 - e^{-(\bar{q}_s^* + \delta q_s^*)/U^*}\right) (\bar{q}_s^* + \delta q_s^*) - \left(1 - e^{-\bar{M}_s^* - \delta M_s^*}\right) q_t^*$$

1173 (eq. A10)

1174 Again, since the δ variables are small, we can replace the relevant exponentials with Taylor expansion
 1175 to first order:

$$e^{-\delta q_s^*/U^*} \approx 1 - \frac{\delta q_s^*}{U^*}$$

1176

1177 (eq. A11)

1178 A similar approximation applies for the exponential in M_s^* . Substituting eq. (A11) into eq. (A10),
 1179 expanding the multiplicative terms, dropping terms of second order in the δ variables and
 1180 rearranging, we get

$$\frac{\partial \delta M_s^*}{\partial t^*} = \delta q_s^* \left(1 - e^{-\bar{q}_s^*/U^*} + \frac{\bar{q}_s^*}{U^*} e^{-\bar{q}_s^*/U^*} \right) - \delta M_s^* \left(q_t^* - \left(1 - e^{-\bar{q}_s^*/U^*} \right) \bar{q}_s^* \right)$$

1181

1182 (eq. A12)

1183 The perturbation is assumed to be sinusoidal

$$\delta q_s^* = d \sin\left(\frac{2\pi t}{p}\right)$$

1184

1185 (eq. A13)

1186 Here, p is the period of the perturbation and d is its amplitude. Note that, to be consistent with the
 1187 assumptions previously made, d needs to be small in comparison with the average sediment supply.
 1188 Substituting, eq. (A12) can be integrated to obtain the solution

$$\delta M_s^* = G_{q_s^*} \sin\left(\frac{2\pi t}{p} + \varphi_{q_s^*}\right) + C \exp\left\{-\left(q_t^* - \left(1 - e^{-\bar{q}_s^*/U^*}\right) \bar{q}_s^*\right) \frac{t}{T}\right\}$$

1189

1190 where C is a constant of integration. The gain is given by

$$G_{q_s^*} = \frac{p}{T} \frac{\left(1 - e^{-\bar{q}_s^*/U^*} + \frac{\bar{q}_s^*}{U^*} e^{-\bar{q}_s^*/U^*}\right) d}{\sqrt{\left(q_t^* - \left(1 - e^{-\bar{q}_s^*/U^*}\right) \bar{q}_s^*\right)^2 \left(\frac{p}{T}\right)^2 + 4\pi^2}}$$

1191

1192 (eq. A14)

1193 And the phase shift by

$$\varphi_{q_s^*} = \tan^{-1} \left[-\frac{2\pi}{\frac{p}{T} \left(q_t^* - \left(1 - e^{-\bar{q}_s^*/U^*} \right) \bar{q}_s^* \right)} \right]$$

1194

1195 (eq. A15)

1196

1197 **Perturbation of transport capacity**

1198

1199 The perturbation of the transport capacity q_t^* is a little more complicated, since both q_t^* and U^* are
 1200 explicitly dependent on hydraulics (e.g., shear stress; see eqs. 43 and 44), and thus U^* is implicitly
 1201 dependent on q_t^* and δq_t^* . To circumvent this problem, we expand the exponential term featuring
 1202 $U^*(\delta q_t^*)$ in eq. (A9) using a Taylor series expansion around $\delta q_t^* = 0$.

1203

$$\exp\left\{-\frac{q_s^*}{U^*(\delta q_t^*)}\right\} \approx \exp\left\{-\frac{q_s^*}{U^*(\delta q_t^* = 0)}\right\} \left[1 - \frac{q_s^*}{U^{*2}(\delta q_t^* = 0)} \frac{\partial U^*}{\partial \delta q_t^*} (\delta q_t^* = 0) \delta q_t^* \right]$$

1204

1205 (eq. A16)

1206 Both U^* and its derivative are constants when evaluated at $\delta q_t^* = 0$. We can thus write

1207

$$\exp\left\{-\frac{q_s^*}{U^*}\right\} = \exp\left\{-\frac{q_s^*}{U^*}\right\} \left[1 - \frac{q_s^*}{U^{*2}} \left(\frac{\partial U^*}{\partial \delta q_t^*} \right) \delta q_t^* \right] = [1 - C_0 \delta q_t^*] e^{-q_s^*/U^*}$$

1208

1209

1210 (eq. A17)

1211 Here, C_0 is a constant. Proceeding as before by substituting eq. (A2), (A8) and (A17) into (A9),
 1212 expanding exponential terms containing δ variables, dropping terms of second order in the δ
 1213 variables and rearranging, we obtain:

$$1214 \quad \frac{\partial \delta M_s^*}{\partial t^*} = \left(B q_s^* e^{-q_s^*/U^*} + e^{-\overline{M_s^*}} - 1 \right) \delta q_t^* - \delta M_s^* \overline{q_t^*} e^{-\overline{M_s^*}}$$

1215 (eq. A18)

1216 A sinusoidal perturbation of the form

$$1217 \quad \delta q_t^* = d \sin\left(\frac{2\pi t}{p}\right)$$

1218 (eq. A19)

1219 yields the solution

$$1220 \quad \delta M_s^* = G_{q_t^*} \sin\left(\frac{2\pi t}{p} + \varphi_{q_t^*}\right) + C \exp\left\{-\left(\overline{q_t^*} - \left(1 - e^{-q_s^*/U^*}\right) q_s^*\right) \frac{t}{p}\right\} \left\{-\left(\overline{q_t^*} - \left(1 - e^{-q_s^*/U^*}\right) q_s^*\right) \frac{t}{T}\right\}$$

1221 with

$$1222 \quad G_{q_t^*} = \frac{p \left(\frac{q_s^{*2}}{U^{*2}} \overline{\left(\frac{\partial U^*}{\partial \delta q_t^*}\right)} e^{-q_s^*/U^*} - \left(1 - e^{-q_s^*/U^*}\right) \frac{q_s^*}{q_t^*} \right) d}{\sqrt{\overline{q_t^*}^2 \left(\frac{p}{T}\right)^2 \left(1 - \left(1 - e^{-q_s^*/U^*}\right) \frac{q_s^*}{q_t^*}\right)^2 + 4\pi^2}}$$

1223 (eq. A20)

1224 and

$$1225 \quad \varphi = \tan^{-1} \left(-\frac{2\pi}{\frac{p}{T} \left(\overline{q_t^*} - \left(1 - e^{-q_s^*/U^*}\right) q_s^* \right)} \right)$$

1226 (eq. A21)

1227

1228 **Summary**

1229

1230 Using the system timescale T_s , the phase shift and gain can be generally rewritten as

1231

$$1232 \quad \varphi = \tan^{-1} \left(-2\pi \frac{T_s}{p} \right)$$

1233 (eq. A22)

$$1234 \quad G = \frac{p}{T_s} \frac{Kd}{\sqrt{\left(\frac{p}{T_s}\right)^2 + 4\pi^2}}$$

1235 (eq. A23)

1236 Here, K differs for perturbations in sediment supply and transport capacity, given by the equations

1237

$$1238 \quad K_{q_s^*} = 1 - e^{-\overline{q_s^*}/U^*} + \frac{\overline{q_s^*}}{U^*} e^{-\overline{q_s^*}/U^*}$$

1239 (eq. A24)

$$1240 \quad K_{q_t^*} = \frac{q_s^{*2}}{U^{*2}} \overline{\left(\frac{\partial U^*}{\partial \delta q_t^*}\right)} e^{-q_s^*/U^*} - \left(1 - e^{-q_s^*/U^*}\right) \frac{q_s^*}{q_t^*}$$

1241 (eq. A25)

1242

1243

1244 **Notation**

1245

1246 Overbars denote time-averaged quantities.

1247

1248 a Shape parameter in the regularized incomplete Beta function.

1249 A^* Fraction of exposed (uncovered) bed area.

1250 A_c^* Fraction of covered bed area.

1251 b Shape parameter in the regularized incomplete Beta function.

1252 B Regularized incomplete Beta function.

1253 C Constant of integration.

1254 C_0 Constant [m^2s/kg].

1255 d Amplitude of perturbation [kg/m^2s].

1256 D Sediment deposition rate per bed area [kg/m^2s].

1257 D_{tot} **Sediment deposition rate [kg/s].**

1258 D^* Dimensionless sediment deposition rate.

1259 D_{50} Median grain size [m].

1260 e Base of the natural logarithm.

1261 E Sediment entrainment rate per bed area [kg/m^2s].

1262 E_{tot} **Sediment entrainment rate [kg/s].**

1263 E^* Dimensionless sediment entrainment rate.

1264 E_{max} Maximal possible dimensionless sediment entrainment rate.

1265 g Acceleration due to gravity [m/s^2].

1266 G Gain [kg/m^2s].

1267 I Non-dimensional incision rate.

1268 k Probability of sediment deposition on uncovered parts of the bed, linear implementation.

1270 k_I Non-dimensional erodibility.

1271 K Parameter in the gain equation.

1272 L Characteristic length scale [m].

1273 M_0 Minimum mass per area necessary to cover the bed [kg/m^2].

1274 M_0^* Dimensionless characteristic sediment mass.

1275 M_m Mobile sediment mass [kg/m^2].

1276 M_m^* Dimensionless mobile sediment mass.

1277 M_s Stationary sediment mass [kg/m^2].

1278 M_s^* Dimensionless stationary sediment mass.

1279 p Period of perturbation [s].

1280 p_c Probability of entrainment, CA model, blocked grains.

1281 p_i Probability of entrainment, CA model, free grains.

1282 P Probability of sediment deposition on uncovered parts of the bed.

1283 q_s Mass sediment transport rate per unit width [kg/ms].

1284 q_s^* Dimensionless sediment transport rate.

1285 q_t Mass sediment transport capacity per unit width [kg/ms].

1286 q_t^* Dimensionless transport capacity.

1287 Q_s^* Relative sediment supply; sediment transport rate over transport capacity.

1288 Q_t Mass sediment transport capacity [kg/s].

1289 t Time variable [s].

1290 t^* Dimensionless time.

1291 T Characteristic time scale [s].

1292	T_E	Characteristic time scale for sediment entrainment [s].
1293	T_S	Characteristic system time scale [s].
1294	U	Sediment speed [m/s].
1295	U^*	Dimensionless sediment speed.
1296	x	Dimensional streamwise spatial coordinate [m].
1297	x^*	Dimensionless streamwise spatial coordinate.
1298	y	Dummy variable.
1299	α	Exponent.
1300	γ	Fraction of pore space in the sediment.
1301	δ	denotes time-varying component.
1302	<u>Δi_n</u>	<u>Sediment supply rate from upstream direction [kg/s].</u>
1303	<u>ΔM_m</u>	<u>Change in mobile sediment mass [kg].</u>
1304		
1305	<u>Δo_u</u>	<u>Transport rate of sediment leaving into the downstream direction [kg/s].</u>
1306	<u>Δt</u>	<u>Change in time [s].</u>
1307	θ	Shields stress.
1308	θ_c	Critical Shields stress.
1309	ρ	Density of water [kg/m ³].
1310	ρ_s	Density of sediment [kg/m ³].
1311	τ	Bed shear stress [N/m ²].
1312	τ_c	Critical bed shear stress at the onset of bedload motion [N/m ²].
1313		
1314		

1315 **Acknowledgements**

1316

1317 We thank ~~Joel J.~~ Scheingross and ~~Jean J.~~ Braun for insightful discussions and two anonymous
1318 reviewers ~~and associate editor D. Egholm~~ for ~~insightful~~ their comments on ~~a previous version of~~ the
1319 manuscript. The data from the Erlenbach is owned by and is used with permission of the Mountain
1320 Hydrology and Mass Movements Group at the Swiss Federal Research Institute for Forest Snow and
1321 Landscape Research WSL.

1322

1323 **References**

1324

- 1325 Aubert, G., Langlois, V.J., Allemand, P. (2016). Bedrock incision by bedload: Insights from direct
1326 numerical simulations. *Earth Surf. Dynam.*, 4, 327-342, doi: 10.5194/esurf-4-327-2016
- 1327 Beer, A. R., & Turowski, J. M. (2015). Bedload transport controls bedrock erosion under sediment-
1328 starved conditions. *Earth Surface Dynamics*, 3, 291-309, doi: 10.5194/esurf-3-291-2015
- 1329 Beer, A. R., Turowski, J. M., Fritschi, B., Rieke-Zapp, D. H. (2015). Field instrumentation for high-
1330 resolution parallel monitoring of bedrock erosion and bedload transport, *Earth Surface*
1331 *Processes and Landforms*, 40, 530-541, doi: 10.1002/esp.3652
- 1332 Beer, A. R., Kirchner, J. W., Turowski, J. M. (2016). Graffiti for science – erosion painting reveals
1333 spatially variable erosivity of sediment-laden flows, *Earth Surface Dynamics*, 4, 885-894, doi:
1334 10.5194/esurf-4-885-2016
- 1335 Charru, F., Mouilleron, H., Eiff, O. (2004). Erosion and deposition of particles on a bed sheared by a
1336 viscous flow. *J. Fluid Mech.*, 519, 55-80
- 1337 Chatanantavet, P. & Parker, G. (2008). Experimental study of bedrock channel alluviation under
1338 varied sediment supply and hydraulic conditions. *Water Resour. Res.*, 44, W12446, doi:
1339 10.1029/2007WR006581
- 1340 Cook, K.; Turowski, J. M. & Hovius, N. (2013). A demonstration of the importance of bedload
1341 transport for fluvial bedrock erosion and knickpoint propagation. *Earth Surf. Process.*
1342 *Landforms*, 38, 683-695, doi: 10.1002/esp.3313
- 1343 Fernandez Luque, R. & van Beek, R. (1976). Erosion and transport of bed-load sediment. *J. Hydraul.*
1344 *Res.*, 14, 127-144
- 1345 Finnegan, N. J.; Sklar, L. S. & Fuller, T. K. (2007). Interplay of sediment supply, river incision, and
1346 channel morphology revealed by the transient evolution of an experimental bedrock channel.
1347 *Journal of Geophysical Research*, 112, F03S11, doi: 10.1029/2006JF000569
- 1348 Gilbert, G. K. (1877), Report on the geology of the Henry Mountains: Geographical and geological
1349 survey of the Rocky Mountain region, U.S. Gov. Print. Off., Washington, D. C.
- 1350 Hobbey, D. E. J.; Sinclair, H. D.; Mudd, S. M. & Cowie, P. A. (2011). Field calibration of sediment flux
1351 dependent river incision. *J. Geophys. Res.*, 116, F04017, doi: 10.1029/2010JF001935
- 1352 Hodge, R.A. (in press) Sediment processes in bedrock-alluvial rivers: Research since 2010 and
1353 modelling the impact of fluctuating sediment supply on sediment cover. In: Tsutsumi, D. &
1354 Laronne, J. *Gravel-Bed Rivers: Process and Disasters*. Wiley-Blackwell.
- 1355 Hodge, R. A. & Hoey, T. B. (2012). Upscaling from grain-scale processes to alluviation in bedrock
1356 channels using a cellular automaton model. *J. Geophys. Res.*, 117, F01017, doi:
1357 10.1029/2011JF002145
- 1358 Hodge, R. A., T. B. Hoey, and L. S. Sklar (2011), Bedload transport in bedrock rivers: the role of
1359 sediment cover in grain entrainment, translation and deposition, *J. Geophys. Res.*, 116,
1360 F04028, doi: 10.1029/2011JF002032.
- 1361 Hodge, R. A., and T. B. Hoey (2016), A Froude scale model of a bedrock-alluvial channel reach: 2.
1362 Sediment cover, *J. Geophys. Res.*, in press, doi: 10.1002/2015JF003709

1363 Inoue, T., N. Izumi, Y. Shimizu, G. Parker (2014). Interaction among alluvial cover, bed roughness, and
1364 incision rate in purely bedrock and alluvial-bedrock channel. *J. Geophys. Res.*, 119, 2123-
1365 2146, doi: 10.1002/2014JF003133

1366 Inoue, T., T. Iwasaki, G. Parker, Y. Shimizu, N. Izumi, C.P. Stark, J. Funaki (2016). Numerical simulation
1367 of effects of sediment supply on bedrock channel morphology. *J. Hydr. Eng.*, in press, doi:
1368 10.1061/(ASCE)HY.1943-7900.0001124

1369 Johnson, J.P.L. (2014). A surface roughness model for predicting alluvial cover and bed load transport
1370 rate in bedrock channels. *J. Geophys. Res.*, 119, 2147-2173, doi: 10.1002/2013JF003000

1371 Johnson, J. P. & Whipple, K. X. (2007). Feedbacks between erosion and sediment transport in
1372 experimental bedrock channels. *Earth Surf. Process. Landforms*, 32, 1048-1062, doi:
1373 10.1002/esp.1471

1374 Lague, D. (2010), Reduction of long-term bedrock incision efficiency by short-term alluvial cover
1375 intermittency, *J. Geophys. Res.*, 115, F02011, doi: 10.1029/2008JF001210

1376 Lajeunesse, E.; Malverti, L. & Charru, F. (2010). Bed load transport in turbulent flow at the grain
1377 scale: Experiments and modeling. *Journal of Geophysical Research*, 115, F04001

1378 Paola, C. & Voller, V. R. (2005). A generalized Exner equation for sediment mass balance. *J. Geophys.*
1379 *Res.*, 110, F04014

1380 Phillips, C. B., and D. J. Jerolmack (2016). Self-organization of river channels as a critical filter on
1381 climate signals. *Science*, 352, 694-697

1382 Mackin, J. H. (1948). Concept of the graded river. *Geological Society of America Bulletin* 59: 463-512.
1383 doi: 10.1130/0016-7606(1948)59[463:COTGR]2.0.CO;2

1384 Meyer-Peter, E., and R. Mueller (1948), Formulas for bedload transport, in 2nd meeting Int. Assoc.
1385 Hydraulic Structures Res., edited, Stockholm, Sweden.

1386 Molnar P, Densmore AL, McArdell BW, Turowski JM, Burlando P. (2010). Analysis of changes in the
1387 step-pool morphology and channel profile of a steep mountain stream following a large
1388 flood. *Geomorphology* 124: 85–94. DOI. 10.1016/j.geomorph.2010.08.014

1389 Nelson, P. A., and G. Seminara (2011), Modeling the evolution of bedrock channel shape with erosion
1390 from saltating bed load, *Geophys. Res. Lett.*, 38, L17406, doi: 10.1029/2011GL048628

1391 Nelson, P. A., and G. Seminara (2012), A theoretical framework for the morphodynamics of bedrock
1392 channels, *Geophys. Res. Lett.*, 39, L06408, doi: 10.1029/2011GL050806.

1393 Nitsche, M., D. Rickenmann, J.M. Turowski, A. Badoux, J.W. Kirchner, (2011). Evaluation of bedload
1394 transport predictions using flow resistance equations to account for macro-roughness in
1395 steep mountain streams, *Water Resources Research*, 47, W08513, doi:
1396 10.1029/2011WR010645

1397 Rickenmann D, Turowski JM, Fritschi B, Klaiber A, Ludwig A. (2012). Improved sediment transport
1398 measurements in the Erlenbach stream including a moving basket system. *Earth Surface*
1399 *Processes and Landforms* 37: 1000–1011, doi: 10.1002/esp.3225

1400 Sklar, L. S. & Dietrich, W. (1998). River longitudinal profiles and bedrock incision models: Stream
1401 power and the influence of sediment supply. In: *Rivers over Rock: Fluvial Processes in*
1402 *Bedrock Channels*, E. Tinkler, K. J. & Wohl, E. E. (Eds.), American Geophysical Union, 107, 237-
1403 260

1404 Sklar, L. S., Dietrich, W. E., (2001). Sediment and rock strength controls on river incision into bedrock.
1405 *Geology* 29, 1087-1090, doi: 10.1130/0091-7613(2001)029<1087:SARSCO>2.0.CO;2

1406 Sklar, L. S. & Dietrich, W. E. (2004). A mechanistic model for river incision into bedrock by saltating
1407 bed load. *Water Resour. Res.*, 40, W06301, doi: 10.1029/2003WR002496

1408 Turowski, J. M. (2009). Stochastic modeling of the cover effect and bedrock erosion. *Water Resour.*
1409 *Res.*, 45, W03422, doi: 10.1029/2008WR007262

1410 Turowski, J. M. & Bloem, J.-P. (2016). The influence of sediment thickness on energy delivery to the
1411 bed by bedload impacts. *Geodynamica Acta*, 28, 199-208, doi:
1412 10.1080/09853111.2015.1047195

1413 Turowski, J. M. & Rickenmann, D. (2009). Tools and cover effects in bedload transport observations
1414 in the Pitzbach, Austria. *Earth Surf. Process. Landforms*, 34, 26-37, doi: 10.1002/esp.1686

1415 Turowski, J. M.; Lague, D. & Hovius, N. (2007). Cover effect in bedrock abrasion: A new derivation
1416 and its implication for the modeling of bedrock channel morphology *J. Geophys. Res.*, 112,
1417 F04006, doi: 10.1029/2006JF000697

1418 Turowski, J. M.; Hovius, N.; Hsieh, M.-L.; Lague, D. & Chen, M.-C. (2008). Distribution of erosion
1419 across bedrock channels. *Earth Surf. Process. Landforms*, 33, 353-363, doi: 10.1002/esp.1559

1420 ~~Turowski, J.M., Turowski JM,~~ Yager EM, Badoux A, Rickenmann D, Molnar P. (2009). The impact of
1421 exceptional events on erosion, bedload transport and channel stability in a step-pool
1422 channel. *Earth Surface Processes and Landforms* 34: 1661–1673, doi: 10.1002/esp.1855

1423 Turowski, J.M., A. Badoux, J. Leuzinger, R. Hegglin (2013). Large floods, alluvial overprint, and
1424 bedrock erosion. *Earth Surface Processes and Landforms*, 38, 947-958, doi: 10.1002/esp.3341

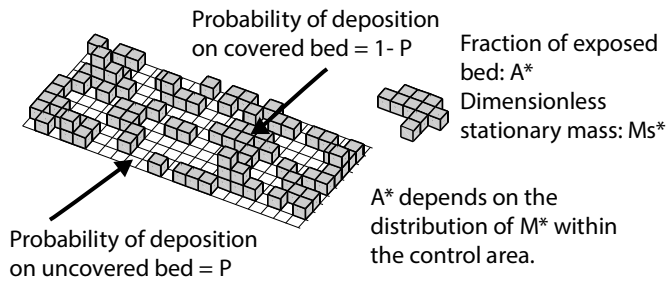
1425 Wohl, E. E. & Ikeda, H. (1997). Experimental simulation of channel incision into a cohesive substrate
1426 at varying gradients. *Geology*, 25, 295-298, doi: 10.1130/0091-
1427 7613(1997)025<0295:ESOCII>2.3.CO;2

1428 Wyss, C.R., D. Rickenmann, B. Fritschi, J.M. Turowski, V. Weitbrecht, R.M. Boes, (2016). Measuring
1429 bedload transport rates by grain-size fraction using the Swiss Plate Geophone signal at the
1430 Erlenbach, *Journal of Hydraulic Engineering*, 142(5), 04016003, doi: 10.1061/(ASCE)HY.1943-
1431 7900.0001090

1432 Yanites, B. J.; Tucker, G. E.; Hsu, H.-L.; Chen, C.-C.; Chen, Y.-G. & Mueller, K. J. (2011). The influence of
1433 sediment cover variability on long-term river incision rates: An example from the Peikang
1434 River, central Taiwan. *J. Geophys. Res.*, 116, F03016, doi: 10.1029/2010JF001933

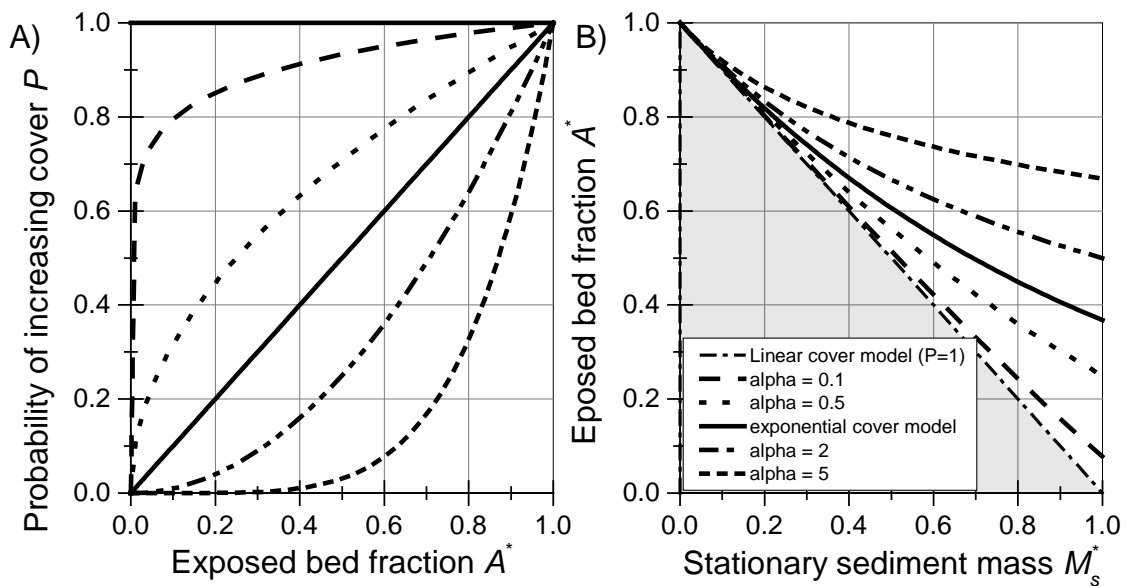
1435 Zhang, L., G. Parker, C.P. Stark, T. Inoue, E. Viparelli, X. Fu, N. Izumi (2015). Macro-roughness model
1436 of bedrock-alluvial river morphodynamics. *Earth Surface Dynamics*, 3, 113-138, doi:
1437 10.5194/esurf-3-113-2015

1438



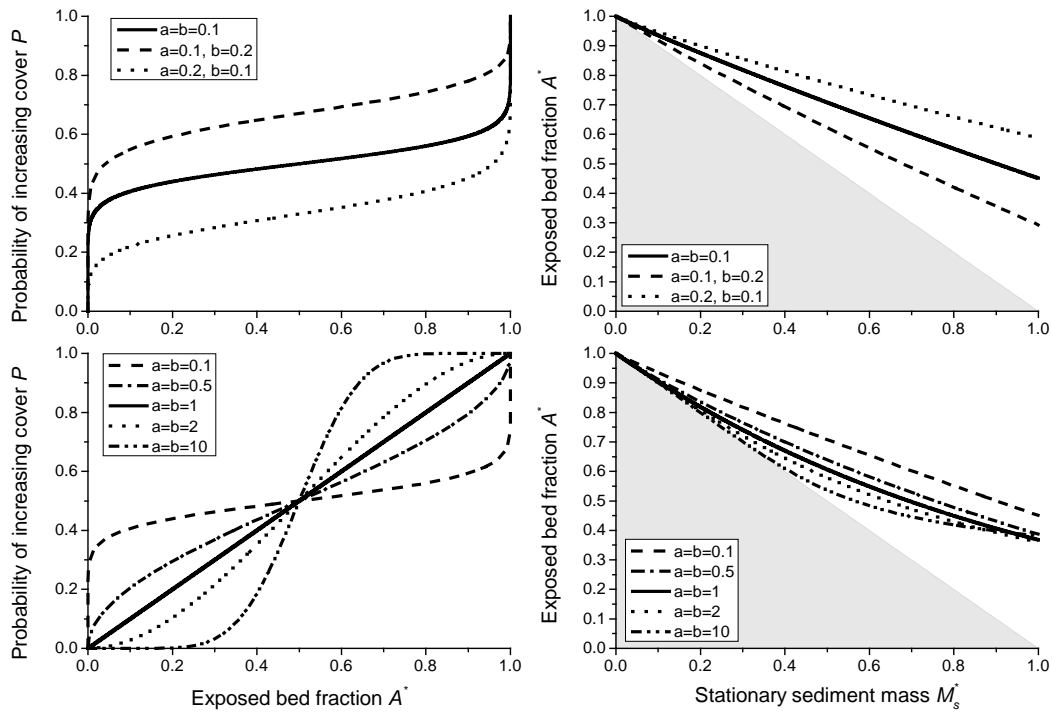
1439
1440
1441
1442
1443
1444

Fig. 1: Cartoon illustration of a bed partially covered by sediment. For purpose of illustration, the bed is divided into a square raster, with each pixel of the size of a single grain. For a given number of particles in the area of the bed of interest, the exposed area fraction of the bed is dependent on the distribution of particles. Grains that sit on top of other grains do not contribute to cover. The probability that a new grain is deposited on uncovered bed is given by P (eq. 3).



1445
1446
1447
1448
1449
1450

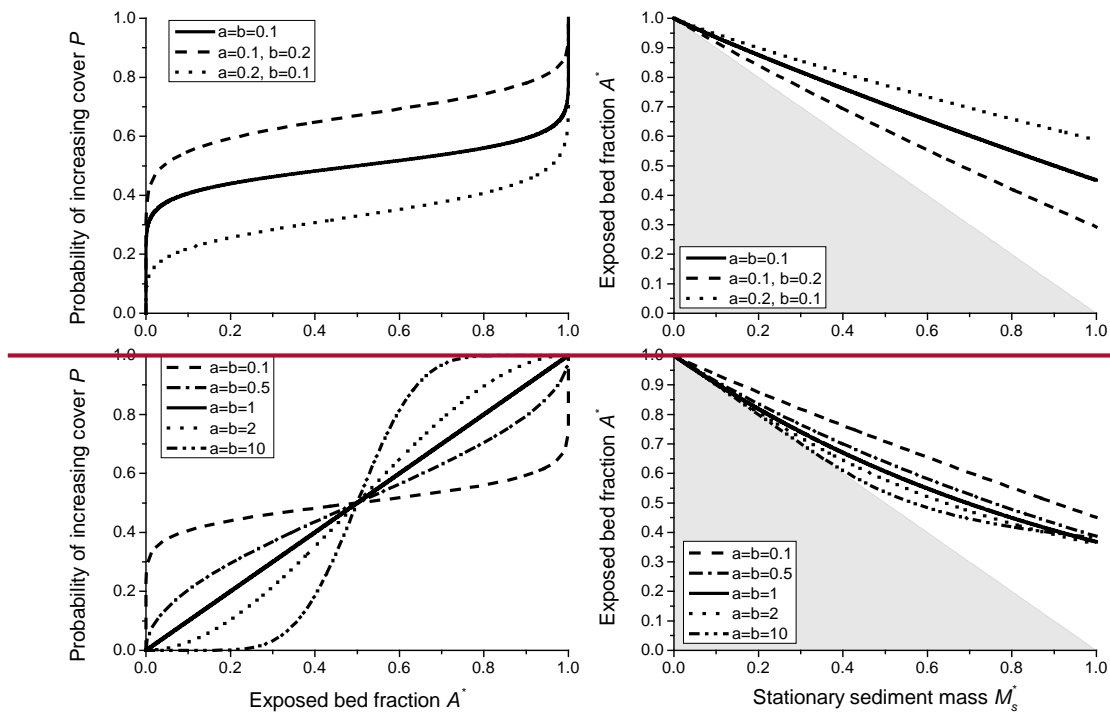
Fig. 2: A) Various examples for the probability function P as a function of bedrock exposure A^* . B) Corresponding analytical solutions for the cover function between A^* and dimensionless sediment mass M_s^* using eq. (6), (7) and (9). Grey shading depicts the area where the cover function cannot run due to conservation of mass.



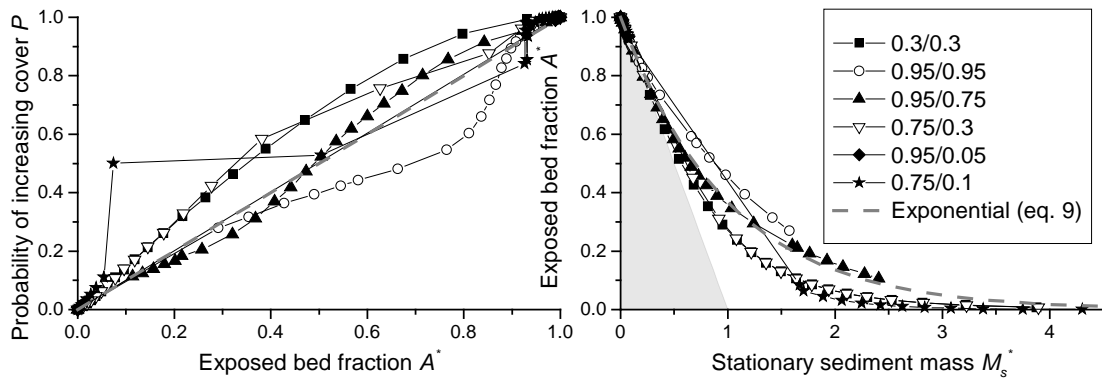
1451
 1452 Fig. 3: Examples for the use of the regularized incomplete Beta function (eq. 11) to parameterize P ,
 1453 using various values for the shape parameters a and b . The choice $a = b = 1$ gives a dependence that
 1454 is equivalent to the exponential cover function. Grey shading depicts the area where the cover
 1455 function cannot run due to conservation of mass.

1456 Fig. 1: A) Various examples for the probability function P as a function of bedrock exposure A^* . B)
 1457 Corresponding analytical solutions for the cover function between A^* and dimensionless sediment
 1458 mass M_s^* using eq. (7), (9) and (10). Grey shading depicts the area where the cover function cannot
 1459 run due to conservation of mass.

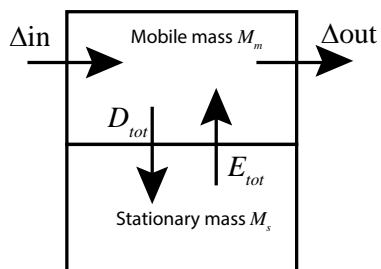
1460



1461
 1462 **Fig. 2:** Examples for the use of the regularized incomplete Beta function (eq. 12) to parameterize P ,
 1463 using various values for the shape parameters a and b . The choice $a = b = 1$ gives a dependence that
 1464 is equivalent to the exponential cover function. Grey shading depicts the area where the cover
 1465 function cannot run due to conservation of mass.

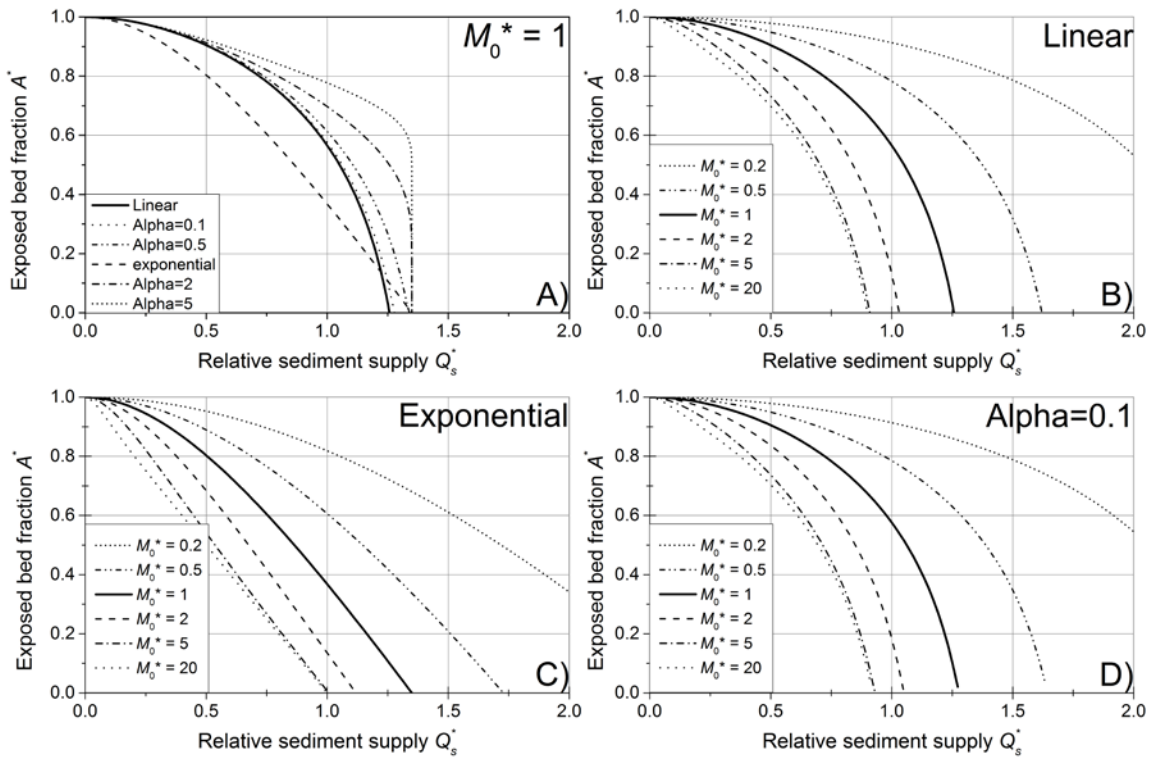


1466
 1467 **Fig. 34:** Probability functions P and cover function derived from data obtained from the model of
 1468 Hodge and Hoey (2012). The grey dashed line shows the exponential benchmark behavior. Grey
 1469 shading depicts the area where the cover function cannot run due to conservation of mass. The
 1470 legend gives values of p_i and p_c used for the runs (see text).
 1471



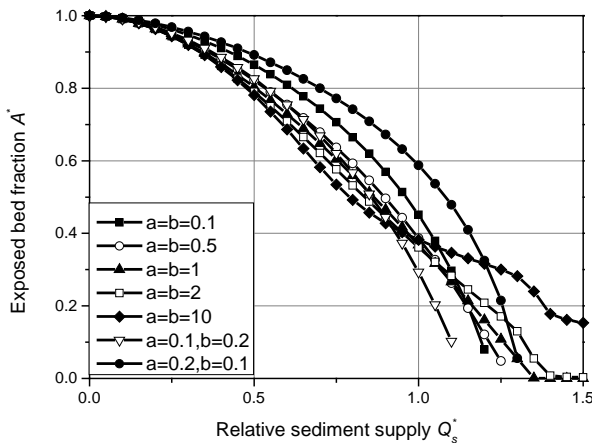
1472

1473 Fig. 5: Sediment dynamics at the bed are modelled by two reservoirs for stationary and mobile mass,
1474 which can exchange material by entrainment (E_{tot}) and deposition (D_{tot}). Sediment mass can be
1475 supplied from upstream (Δ_{in}) and can leave into the downstream direction (Δ_{out}).
1476



1478 Fig. 6: Analytical solutions at steady state for the exposed fraction of the bed (A^*) as a function of
 1479 relative sediment supply (Q_s^* , cf. Fig. 2). A) Comparison of the different solutions, keeping M_0^*
 1480 constant at 1. B) Varying M_0^* for the linear case (eq. 31). C) Varying M_0^* for the exponential case (eq.
 1481 30). D) Varying M_0^* for the power law case with $\alpha = 0.1$ (eq. 32).

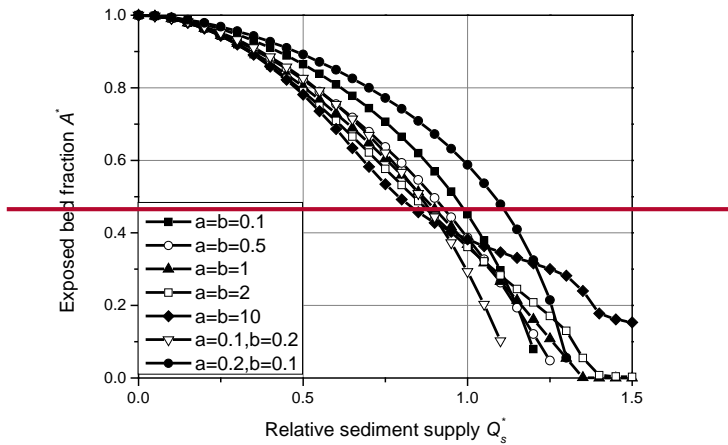
1483



1484 Fig. 7: Steady state solutions using the beta distribution to parameterize P (eq. 10) for a range of
 1485 parameters a and b , and using $M_0^* = 1$ (cf. Fig. 3). The solutions were obtained by iterating the
 1486 equations to a steady state, using initial conditions of $A^* = 1$ and $M_m^* = M_s^* = 0$.
 1487 Fig. 4: Analytical solutions at steady state for the exposed fraction of the bed (A^*) as a function of relative sediment
 1488 supply (Q_s^* , cf. Fig. 1). A) Comparison of the different solutions, keeping M_0^* constant at 1. B) Varying
 1489 M_0^* for the linear case (eq. 31). C) Varying M_0^* for the exponential case (eq. 30). D) Varying M_0^* for
 1490 the power law case with $\alpha = 0.1$ (eq. 32).

1491

1492



1493

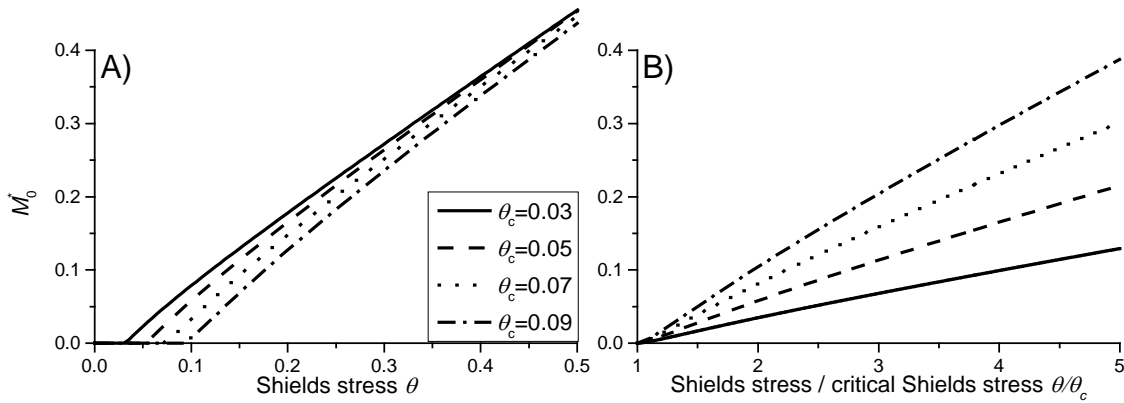
1494

1495

1496

1497

Fig. 5: Steady state solutions using the beta distribution to parameterize P (eq. 11) for a range of parameters a and b , and using $M_0^* = 1$ (cf. Fig. 2). The solutions were obtained by iterating the equations to a steady state, using initial conditions of $A^* = 1$ and $M_{m+}^* = M_s^* = 0$.



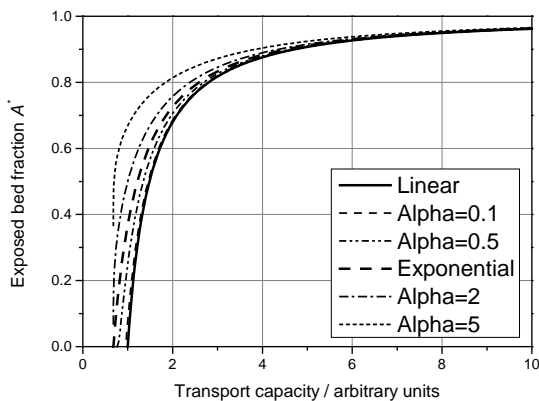
1498

1499

1500

1501

Fig. 8: The characteristic dimensionless mass M_0^* depicted as a function of A) the Shields stress and B) the ratio of Shields stress to critical Shields stress (eq. 37).



1502

1503

1504

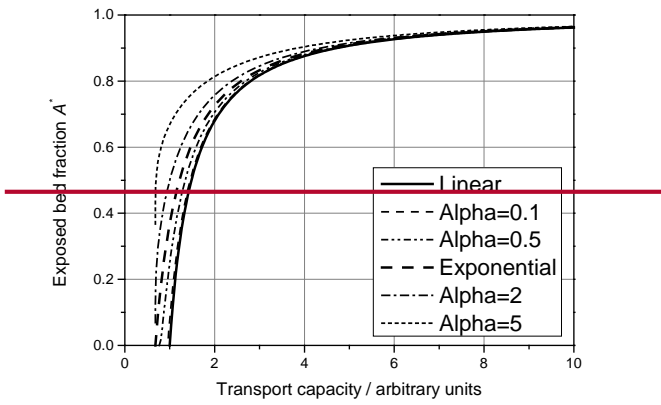
1505

1506

Fig. 9: Variation of the exposed bed fraction as a function of transport capacity, assuming that particle speed scales with transport capacity to the power of one third.

Fig. 6: The characteristic dimensionless mass M_0^* depicted as a function of A) the Shields stress and B) the ratio of Shields stress to critical Shields stress (eq. 37).

1507



1508

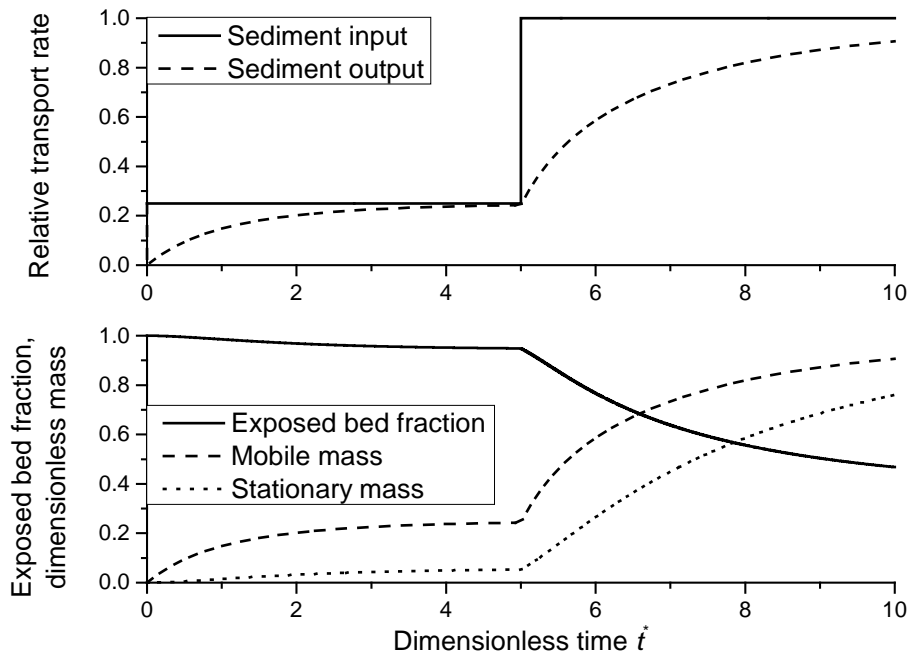
1509

Fig. 7: Variation of the exposed bed fraction as a function of transport capacity, assuming that particle speed scales with transport capacity to the power of one third.

1510

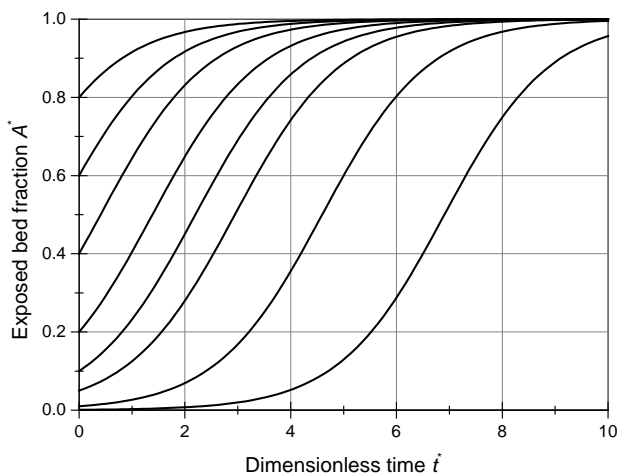
1511

1512



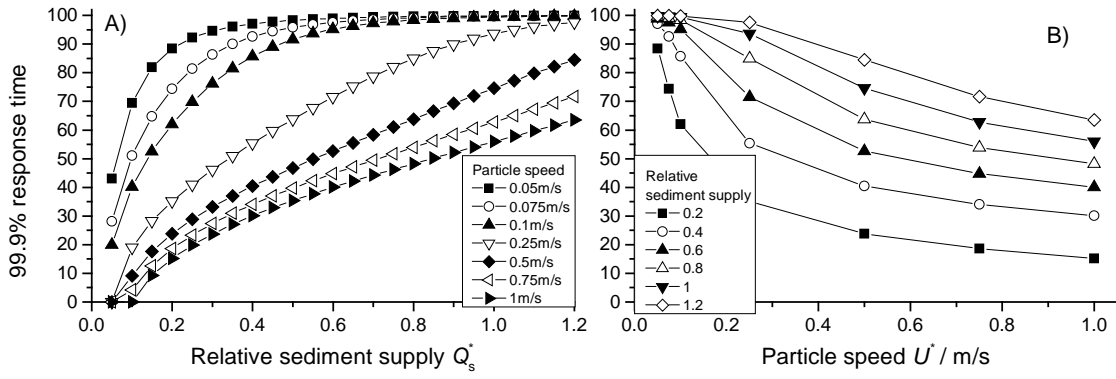
1514
 1515
 1516
 1517
 1518
 1519
 1520
 1521
 1522
 1523
 1524

Fig. 10: Temporal evolution of cover for the simple case of a control box with sediment through-flux, based on eqs. (3), (22), (23) and (24). Relative sediment supply (supply normalized by transport capacity) was specified to 0.25 and increased to 1 at $t^* = 5$. The response of sediment output, mobile and stationary sediment mass and the exposed bed fraction was calculated. Here, we used the exponential function for P (eq. 8) and $M_0^* = U^* = 1$. The initial values were $A^* = 1$ and $M_m^* = M_s^* = 0$.
Fig. 8: Temporal evolution of cover for the simple case of a control box with sediment through-flux, based on eqs. (3), (22), (23) and (24). Relative sediment supply (supply normalized by transport capacity) was specified to 0.25 and increased to 1 at $t^* = 5$. The response of sediment output, mobile and stationary sediment mass and the exposed bed fraction was calculated. Here, we used the exponential function for P (eq. 9) and $M_0^* = U^* = 1$. The initial values were $A^* = 1$ and $M_m^* = M_s^* = 0$.



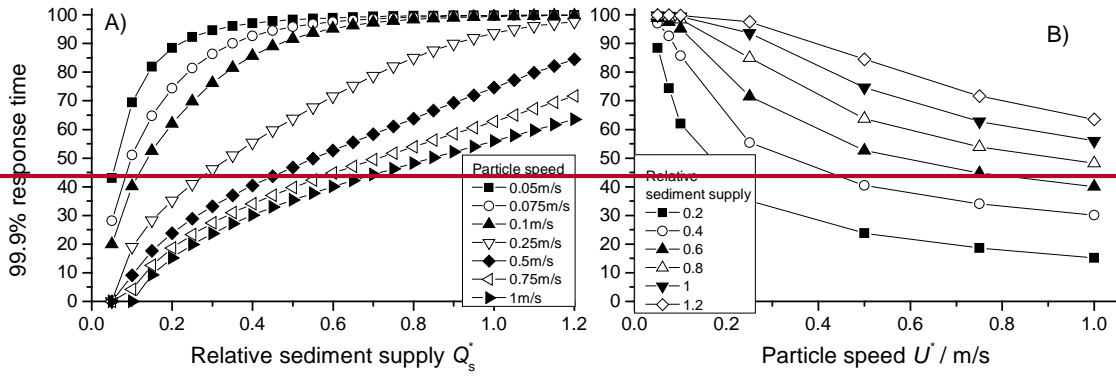
1525
 1526
 1527
 1528
 1529

Fig. 11: Evolution of the exposed bed fraction (removal of sediment cover) over time starting with different initial values of bed exposure, for the special case of no sediment supply, i.e., $q_s^* = 0$ (eq. 41) and $q_t^* = 1$.



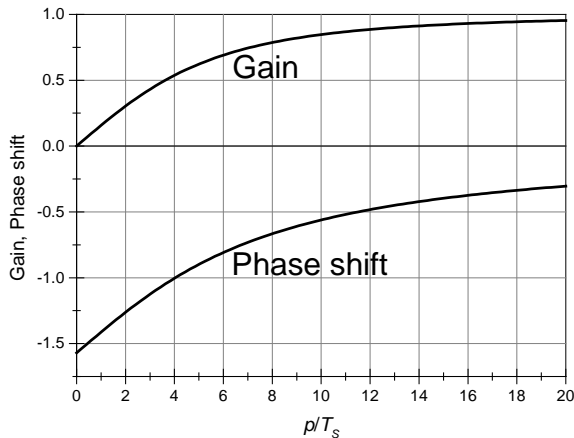
1530
1531
1532
1533
1534
1535
1536

Fig. 12: Dimensionless time to reach 99.9% of the total adjustment in exposed area as a function of A) transport stage and B) particle speed. All simulation were started with $A^* = 1$ and $M_m^* = M_s^* = 0$. Fig. 9: Evolution of the exposed bed fraction (removal of sediment cover) over time starting with different initial values of bed exposure, for the special case of no sediment supply, i.e., $q_s^* = 0$ (eq. 41) and $q_t^* = 1$.



1537
1538
1539
1540

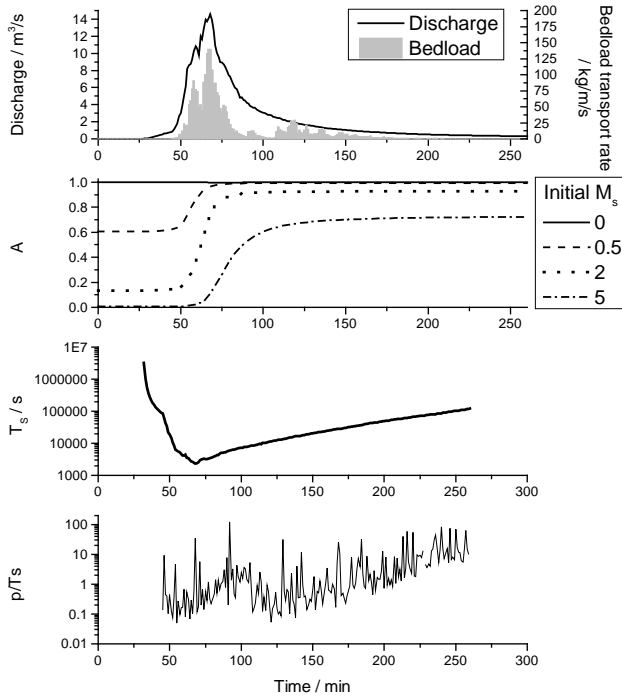
Fig. 10: Dimensionless time to reach 99.9% of the total adjustment in exposed area as a function of A) transport stage and B) particle speed. All simulation were started with $A^* = 1$ and $M_m^* = M_s^* = 0$.



1541
1542
1543
1544

Fig. 13: Phase shift (eq. 49) and gain (eq. 50) as a function of the ratio of the period of perturbation p and the system time scale T_s . For the calculation, the constant factor in the gain (Kd) was set equal to one.

1545 Fig. 11: Phase shift (eq. 50) and gain (eq. 51) as a function of the ratio of the period of perturbation p
 1546 and the system time scale T_s . For the calculation, the constant factor in the gain (K_d) was set equal to
 1547 one.
 1548



1549 Fig. 14: Calculated evolution of cover during the largest event observed at the Erlenbach on 20th June
 1550 2007 (Turowski et al., 2009). Bedload transport rates were measured with the Swiss Plate geophone
 1551 sensors calibrated with direct bedload samples (Rickenmann et al., 2012). The final fraction of
 1552 exposed bedrock is strongly dependent on its initial value.
 1553 Fig. 12: Calculated evolution of cover during the largest event observed at the Erlenbach on 20th June
 1554 2007 (Turowski et al., 2009). Bedload transport rates were measured with the Swiss Plate geophone
 1555 sensors calibrated with direct bedload samples (Rickenmann et al., 2012). The final fraction of
 1556 exposed bedrock is strongly dependent on its initial value.
 1557
 1558